First Result from the Muon g-2 Experiment at Fermilab

S. Di Falco (INFN Pisa)
on behalf of the Muon g-2 collaboration

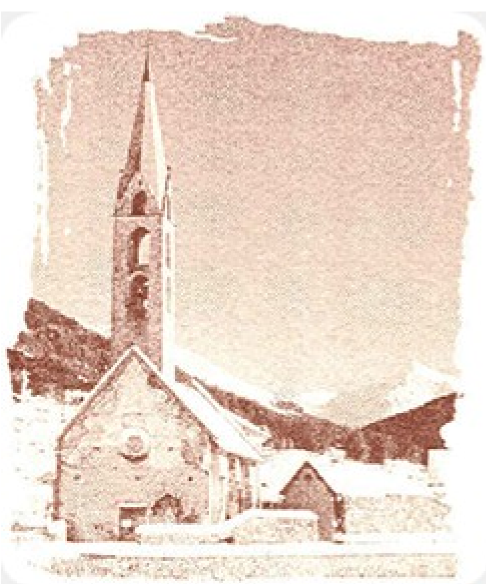

59th International Winter Meeting on Nuclear Physics
January 23 to 27, 2023 Bormio, Italy

The muon anomalous magnetic moment

The muon magnetic moment is proportional to its spin through the **giromagnetic factor g**:

$$\vec{\mu} = \mathbf{g}\frac{q}{2m_\mu}\vec{S}$$

Dirac equation predicts g=2
In 1948, inspired by the ‘anomalous’ results of the experiments on the hyperfine structure of hydrogen and deuterium (1947),

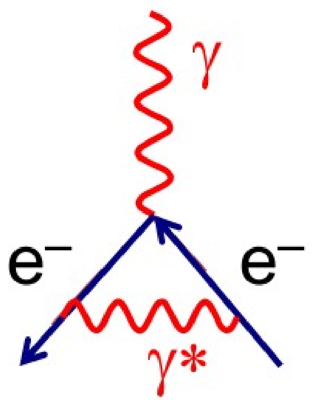

Schwinger calculated the first order QED loop corrections finding:

$$a_\mu = \frac{(g-2)}{2} = \frac{\alpha}{2\pi} = 0.001161$$

THE MUON ANOMALY

In the same year Kush and Foley measured:

$$a_\mu = 0.00119 \pm 0.00005$$

The race between theorists and experimentalists to get the best resolution on a_μ had started!

Standard Model calculation of a_μ

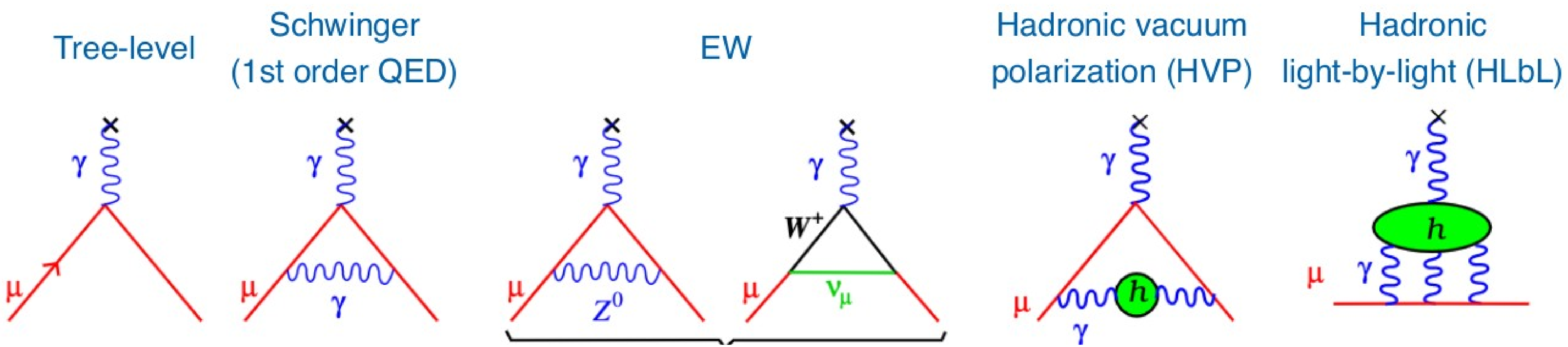

In fact the muon magnetic moment is sensitive to many other non-QED contributions and this makes it an excellent probe to new physics beyond SM

QED contribution remains dominant has the lowest uncertainty (has been calculated up to the 5th order!). The largest theoretical error is due to the hadronic part

Source	Value (x 10^{-11}) [1]	Error
QED	116,584,718.93	0.10
EW	153.6	1.0
HVP	6845	40
HLbL	92	18

[1] T. Aoyama et. al. The anomalous magnetic moment of the muon in the Standard Model (2020).

50 years of experiments on aμ

±	Measurement	σ_{a_μ}/a_μ	Sensitivity	Reference
μ^+	$g = 2.00 \pm 0.10$		$g = 2$	Garwin *et al*[30], Nevis (1957)
μ^+	$0.001\,13^{+0.00016}_{-0.00012}$	12.4%	$\frac{\alpha}{\pi}$	Garwin *et al*[33], Nevis (1959)
μ^+	0.001 145(22)	1.9%	$\frac{\alpha}{\pi}$	Charpak *et al*[34] CERN 1 (SC) (1961)
μ^+	0.001 162(5)	0.43%	$(\frac{\alpha}{\pi})^2$	Charpak *et al*[35] CERN 1 (SC) (1962)
$\mu^\pm$	0.001 166 16(31)	265 ppm	$(\frac{\alpha}{\pi})^3$	Bailey *et al*[36] CERN 2 (PS) (1968)
μ^+	0.001 060(67)	5.8%	$\frac{\alpha}{\pi}$	Henry*et al*[46] solenoid (1969)
$\mu^\pm$	0.001 165 895(27)	23 ppm	$(\frac{\alpha}{\pi})^3$ + Hadronic	Bailey *et al*[37] CERN 3 (PS) (1975)
$\mu^\pm$	0.001 165 911(11)	7.3 ppm	$(\frac{\alpha}{\pi})^3$ + Hadronic	Bailey *et al*[38] CERN 3 (PS) (1979)
μ^+	0.001 165 919 1(59)	5 ppm	$(\frac{\alpha}{\pi})^3$ + Hadronic	Brown *et al*[48] BNL (2000)
μ^+	0.001 165 920 2(16)	1.3 ppm	$(\frac{\alpha}{\pi})^4$ + Weak	Brown *et al*[49] BNL (2001)
μ^+	0.001 165 920 3(8)	0.7 ppm	$(\frac{\alpha}{\pi})^4$ + Weak + ?	Bennett *et al*[50] BNL (2002)
μ^-	0.001 165 921 4(8)(3)	0.7 ppm	$(\frac{\alpha}{\pi})^4$ + Weak + ?	Bennett *et al*[51] BNL (2004)
$\mu^\pm$	0.001 165 920 80(63)	0.54 ppm	$(\frac{\alpha}{\pi})^4$ + Weak + ?	Bennett *et al*[51, 26] BNL WA (2004)

J. Miller, E. De Rafael, L. Roberts, Rept. Prog. Phys. 70 (2007) 795

The **storage ring method**, developed at Cern and perfectioned at Brookhaven has allowed to lower the experimental error to 540 ppb (parts per billion)!

Experimental sensitivity to Standard Model

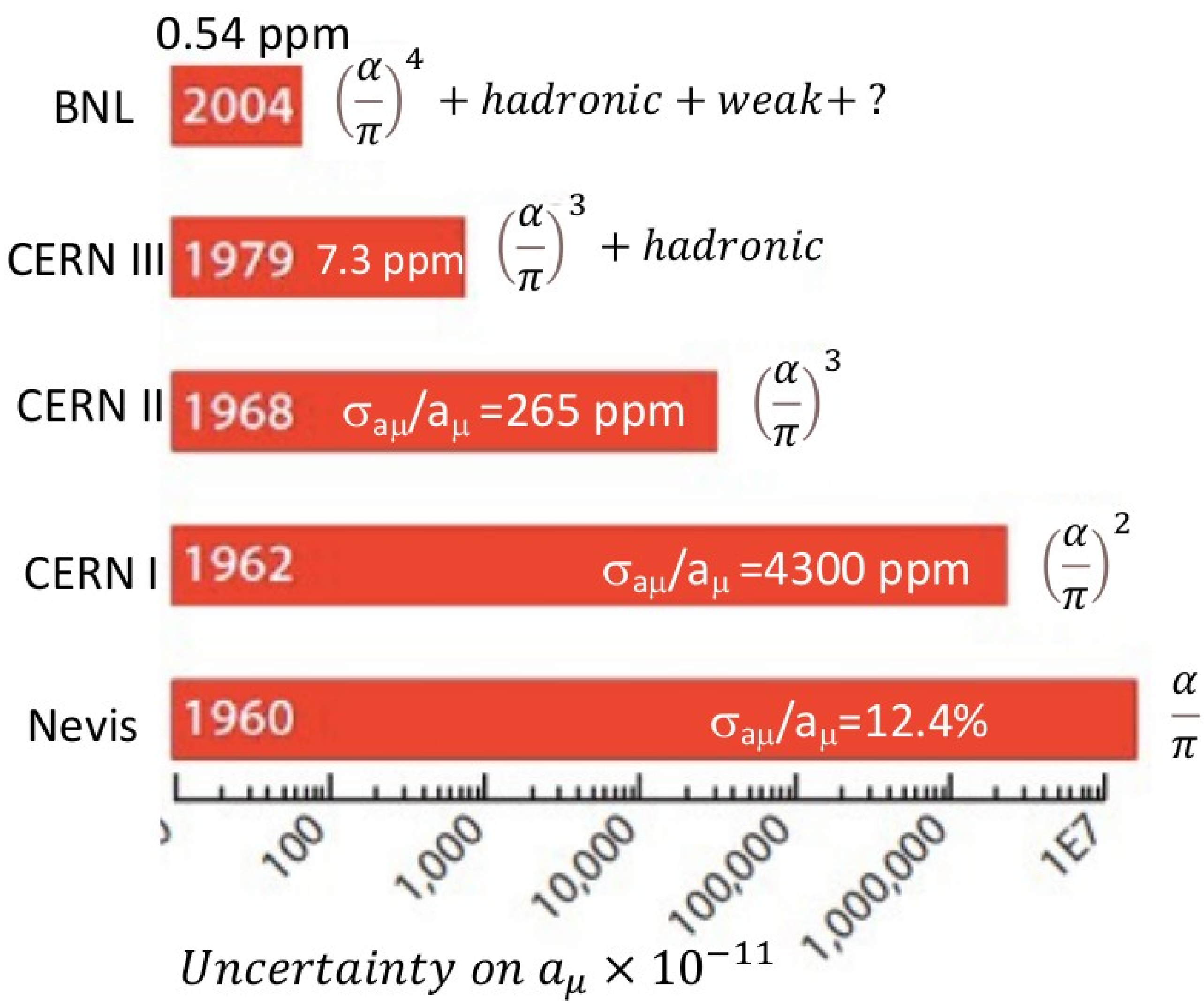

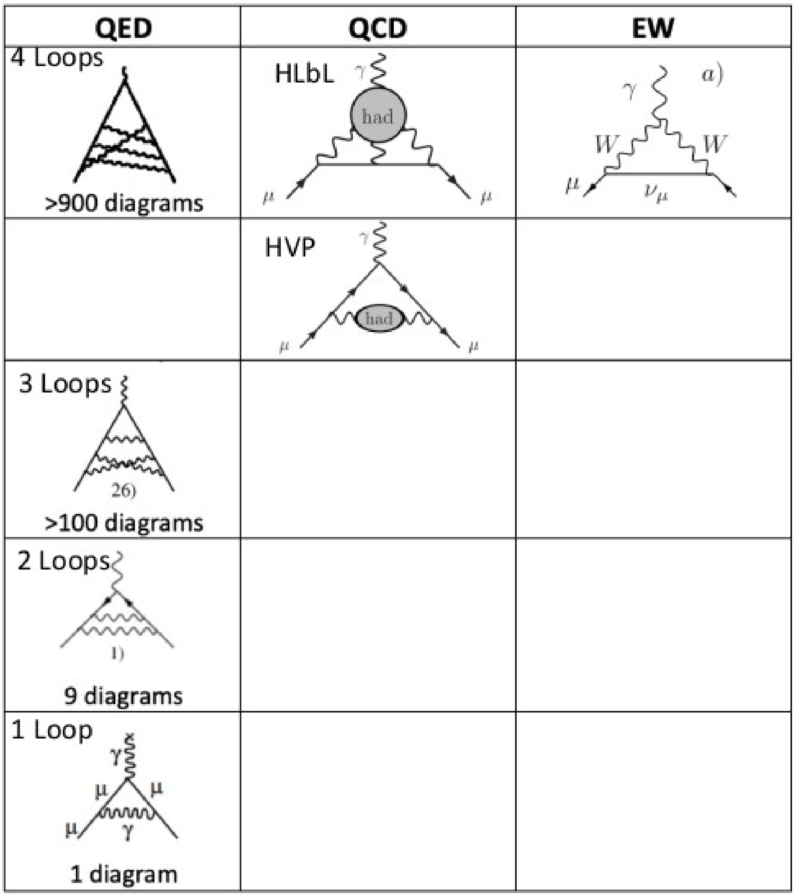

The latest experiments have reached the sensitivity needed to test the QCD and the electroweak contribution

... and maybe something more...

Experiment and theory (before the Muon g-2 result)

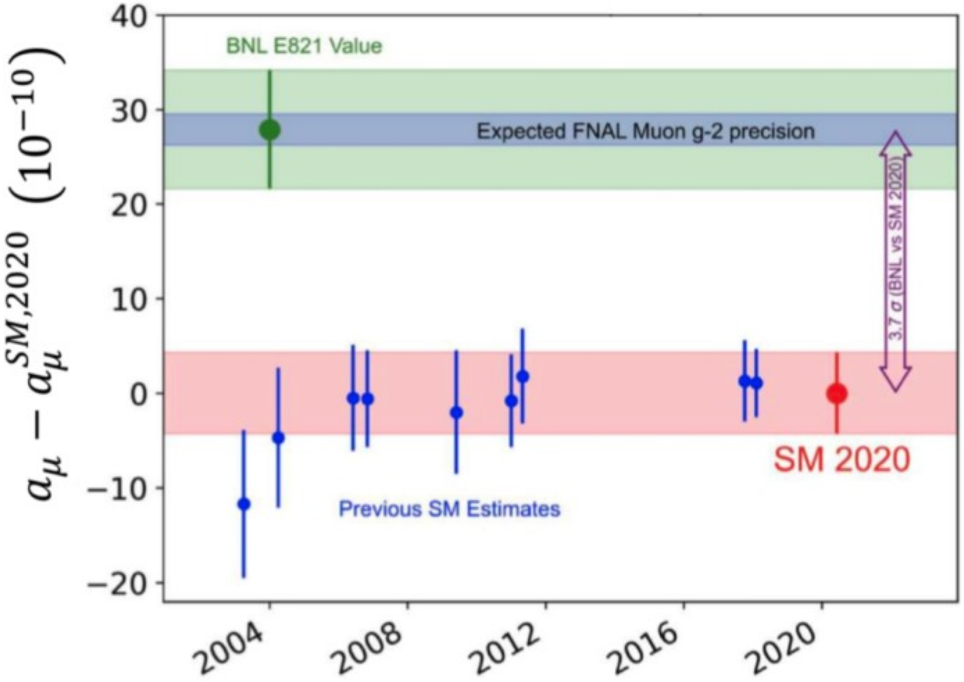

- **E821 (BNL)** experimental value:

$$\boxed{a_\mu^{E821,BNL} = 116592080(63) \times 10^{-11}}$$

[Phys. Rev. D, **73** (2006) 072003]

- **SM value** re-evaluated in 2020 by Muon g-2 Theory Initiative:

$$\boxed{a_\mu^{SM,2020} = 116591810(43) \times 10^{-11}}$$

[Phys. Rept. **887**, 1 (2020)]

Considering the 2020 best theoretical estimate, the BNL E821 result differs from the theory by **3.7σ**

Brookhaven experimental precision was **statistically dominated** (460 out of 540 ppb). This brought the idea to move the BNL storage ring to Fermilab to exploit the intense muon beam provided by the FNAL accelerator.

Also the E821 sytematic error (280 ppb) needs to be improved to reach the muon g-2 goal improvement of x4 BNL

The storage ring method

Muons are stored in a ring with a static magnetic field

If g=2 the momentum rotation frequency (aka cyclotron frequency, ω_c) is the same of the spin one (ω_s). If spin and momentum are aligned at the beginning (polarized muon beam), they stay aligned all the time

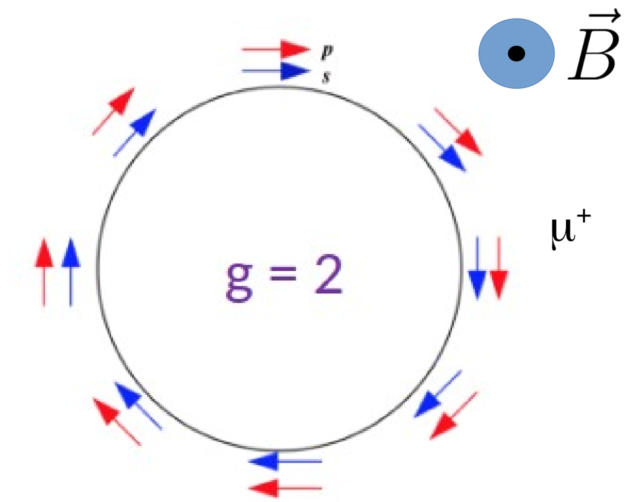

If instead g≠2 we have $\omega_s \neq \omega_c$ and the spin precesses around the momentum with the ‘anomalous’ frequency

$$\vec{\omega}_a = \vec{\omega}_s - \vec{\omega}_c = -a_\mu \frac{q\vec{B}}{m}$$

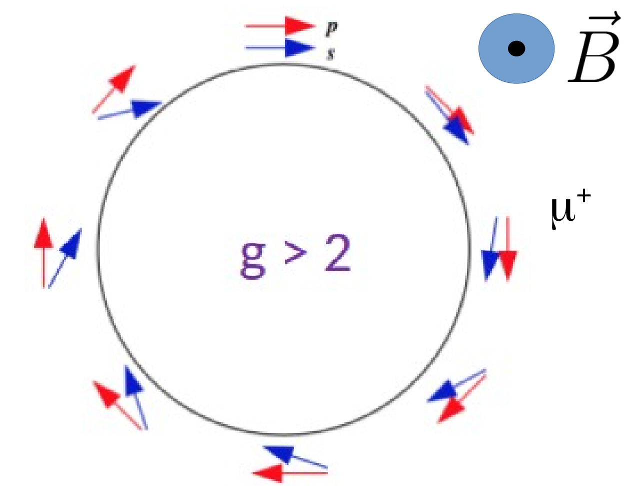

Measuring ω_a and B we can get a_μ
(~800 times more powerful than measurement at rest)

Basics of ω_a measurement

Stored muons decay as usual via $\mu^+ -> e^+ \nu_e \bar{\nu}_\mu$

In the muon rest frame the highest energy e^+ are produced in direction opposite to the two neutrinos

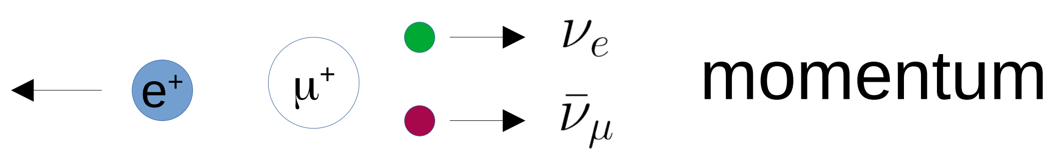

(Anti)Neutrinos have helicity (+1)-1. Given its high momentum [O(GeV/c)] the positron can be considered to have helicity +1. Angular momentum conservation requires the muon spin to be in the direction of the positron spin

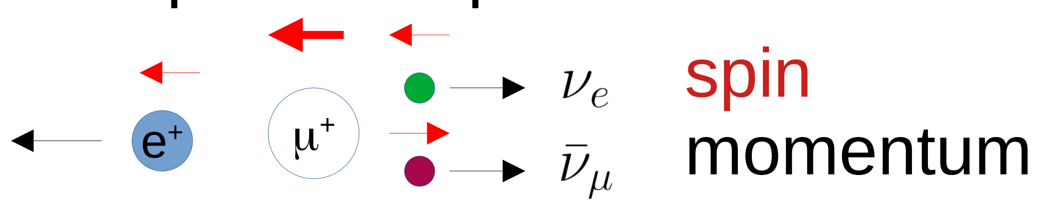

So the highest energy positrons are emitted in the direction of muon spin. Considering then the Lorentz boost, the highest positron energy is obtained when the muon momentum and spin are aligned.

In general the e^+ spectrum in the lab frame depends on the relative alignment between muon spin and momentum, that is on ω_a!

The wiggle plot

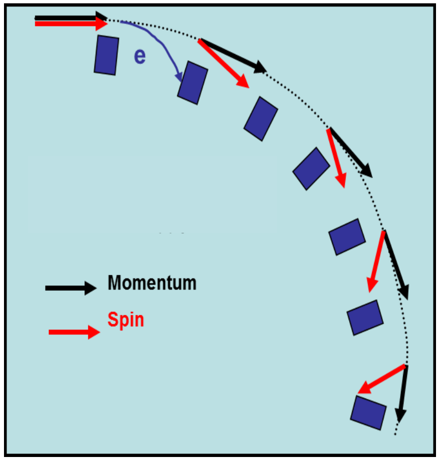

The emitted positrons have a momentum lower than the parent muon and so spiralize inside the ring where they can be detected by a set of calorimeters

The wiggle plot

The emitted positrons have a momentum lower than the parent muon and so they spiralize inside the ring where they can be detected by a set of calorimeters

The calorimeters acceptance selects a fixed range of positron directions so that the measured positron spectrum changes with the relative orientation of the muon momentum and spin

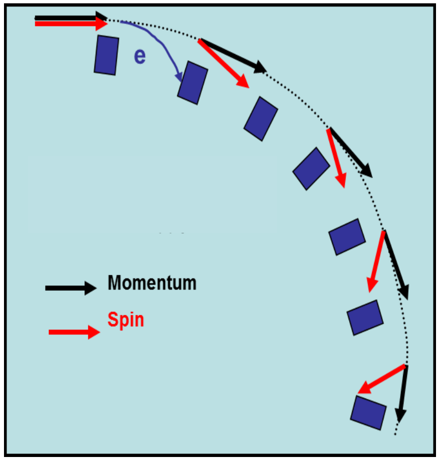

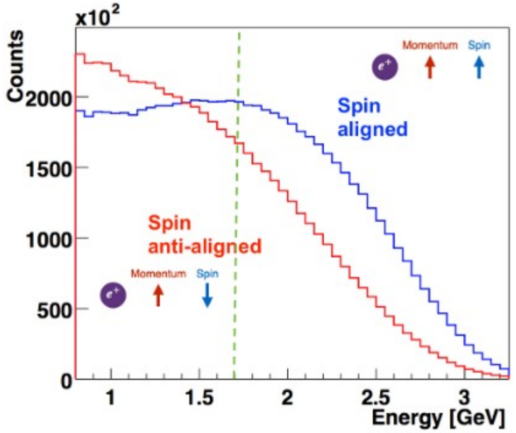

The wiggle plot

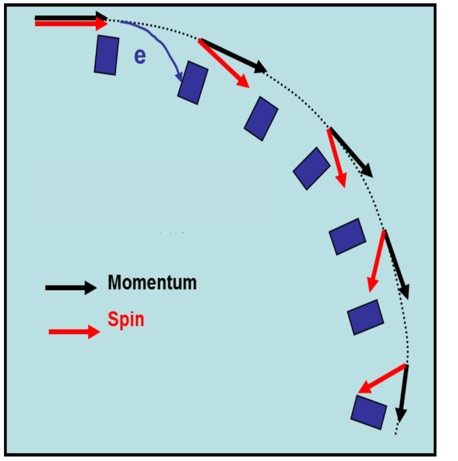

The emitted positrons have a momentum lower than the parent muon and so they spiralize inside the ring where they can be detected by a set of calorimeters

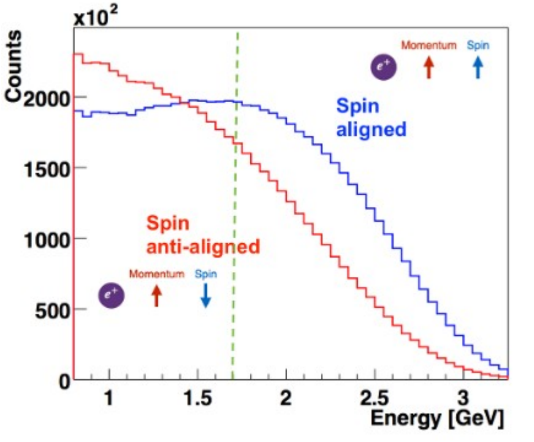

The calorimeters acceptance selects a fixed range of positron directions so that the measured positron spectrum changes with the relative orientation of the muon momentum and spin

The number of positrons above a given threshold (1.7 GeV), follows an exponential (μ decay) modulated by the ω_a frequency (wiggle plot):

$$f(t) \simeq N_0 e^{-\lambda t}[1 + A\cos(\omega_a t + \phi)]$$

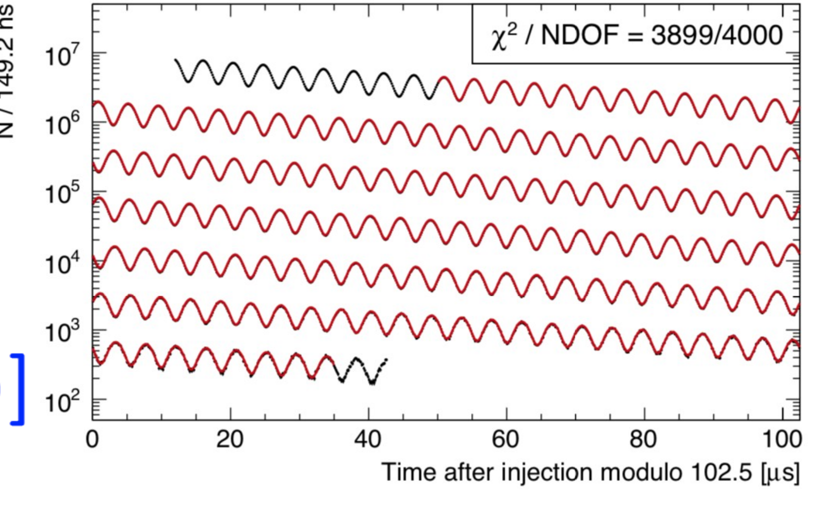

From Brookhaven to Fermilab

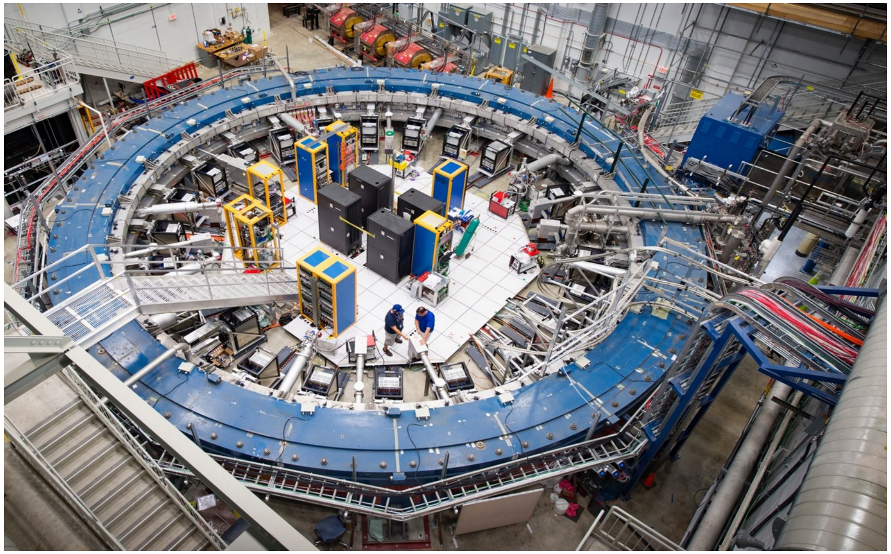

BNL storage ring brought to Fermilab to exploit the intense muon beam provided by the accelerator

An epical journey...

Fermilab muon beam for g-2

- **Recycler Ring:** 8 GeV protons from Booster are divided in 4 bunches
- **Target Station:** p-bunches are collided with target and π^+ with 3.1 GeV/c ($\pm$10%) are collected
- **Beam Transport and Delivery Ring:** magnetic lenses select μ^+ from $\pi^+ \to \mu^+\nu_\mu$ then μ^+ are separated from p and π^+ in circular ring
- **Muon Campus:** polarized μ^+ are ready to be injected into the **storage ring**

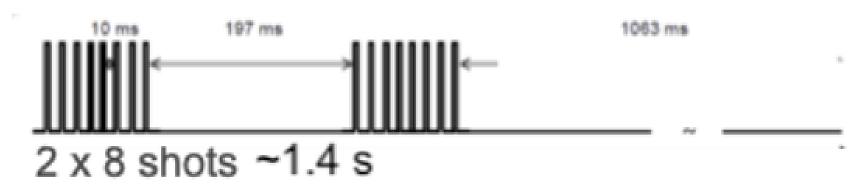

Polarized muon beam arriving to g-2

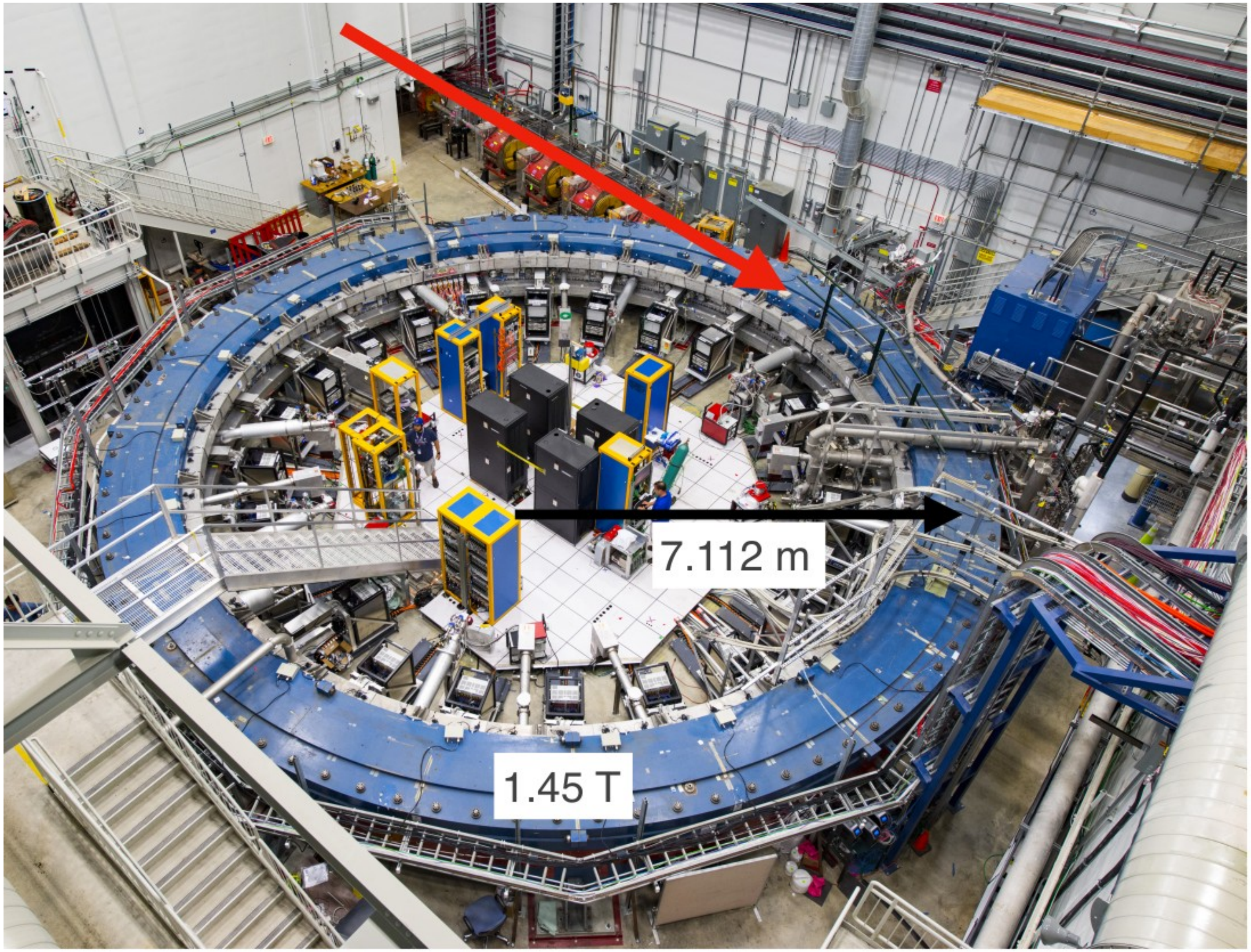

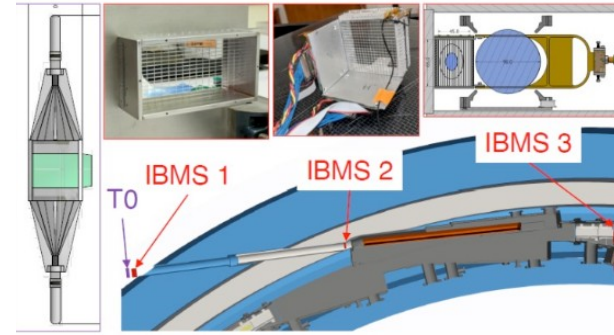

The incoming beam intensity, time profile and spatial distribution are monitored by a plastic scintillator (T_0 detector) and 3 fiber detectors (Injected Beam Monitoring System)

Entering in the ring

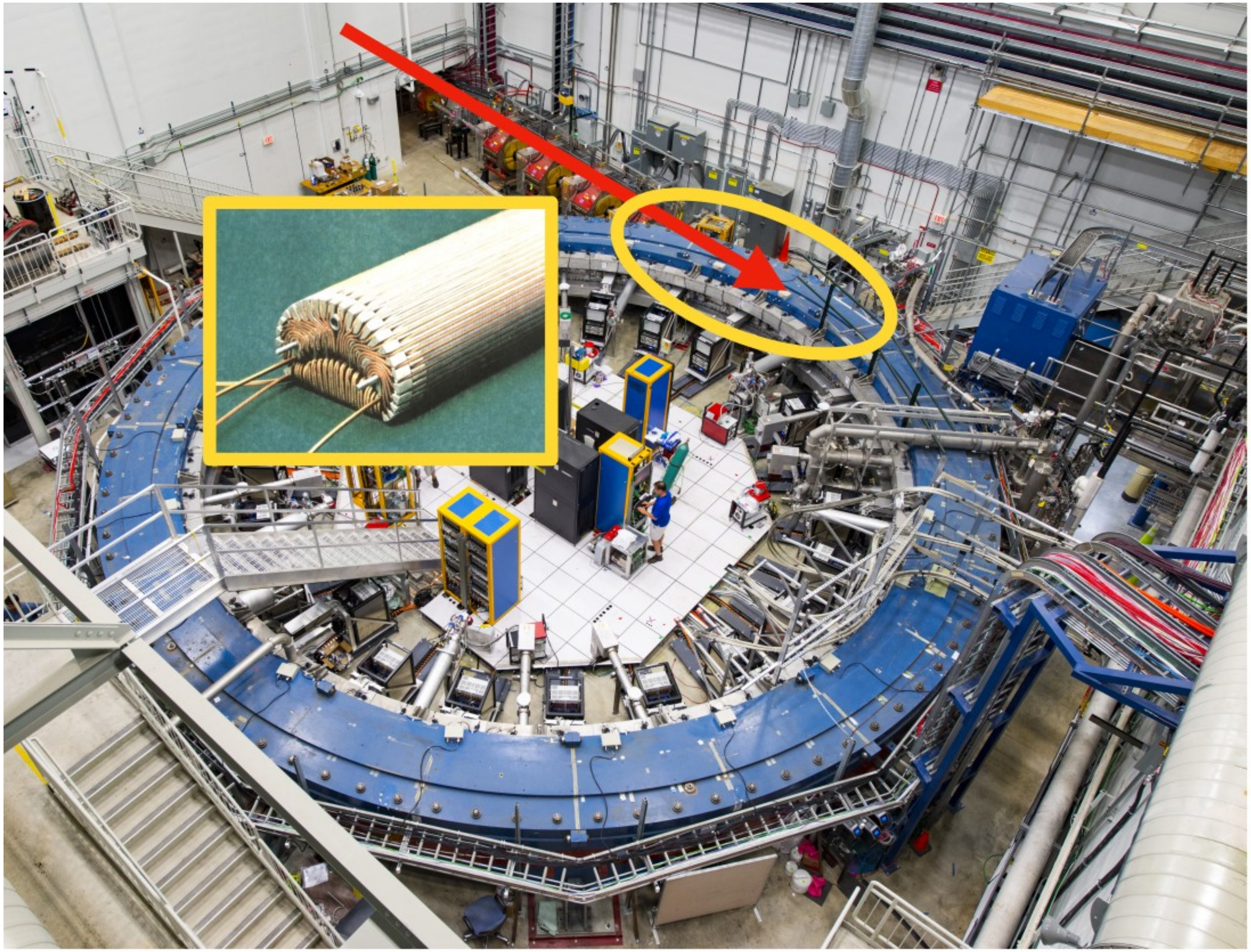

In order to allow the muons to enter in the magnetic ring a 0 field region is created by a superconducting magnet (inflector)

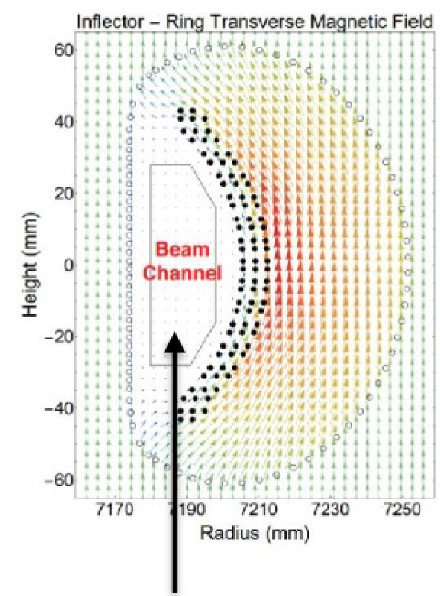

Field free region

Muons ‘kicked’ into the orbit

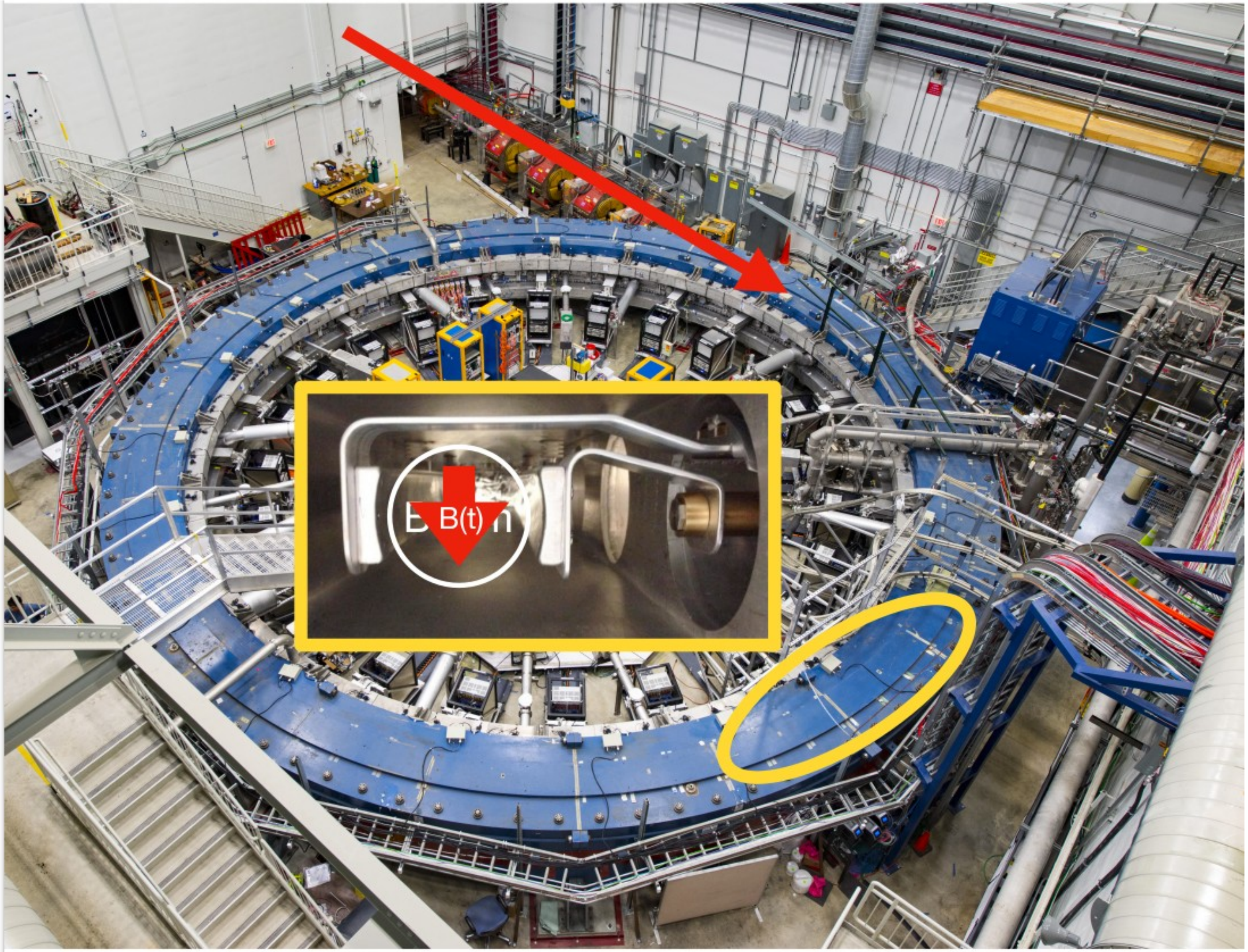

3 magnetic ‘kickers’ push the muons to the wanted orbit

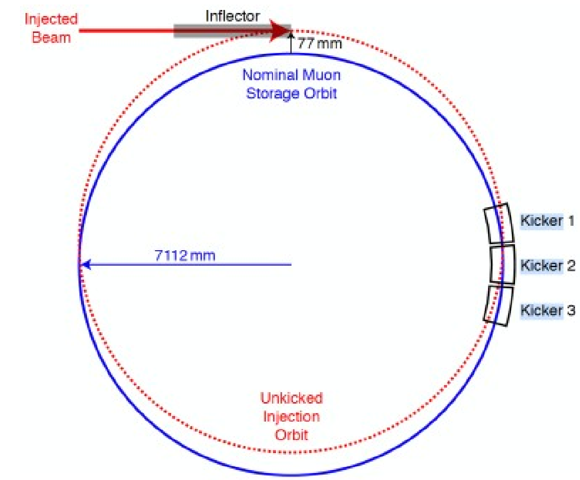

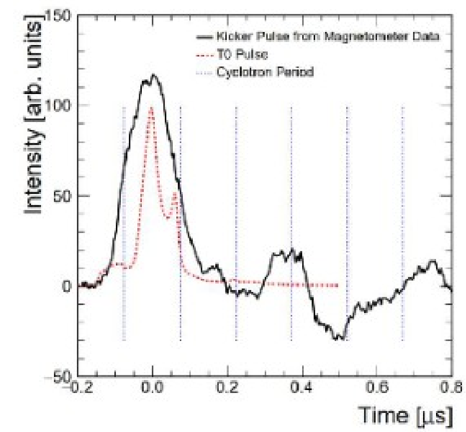

Beam vertical focusing

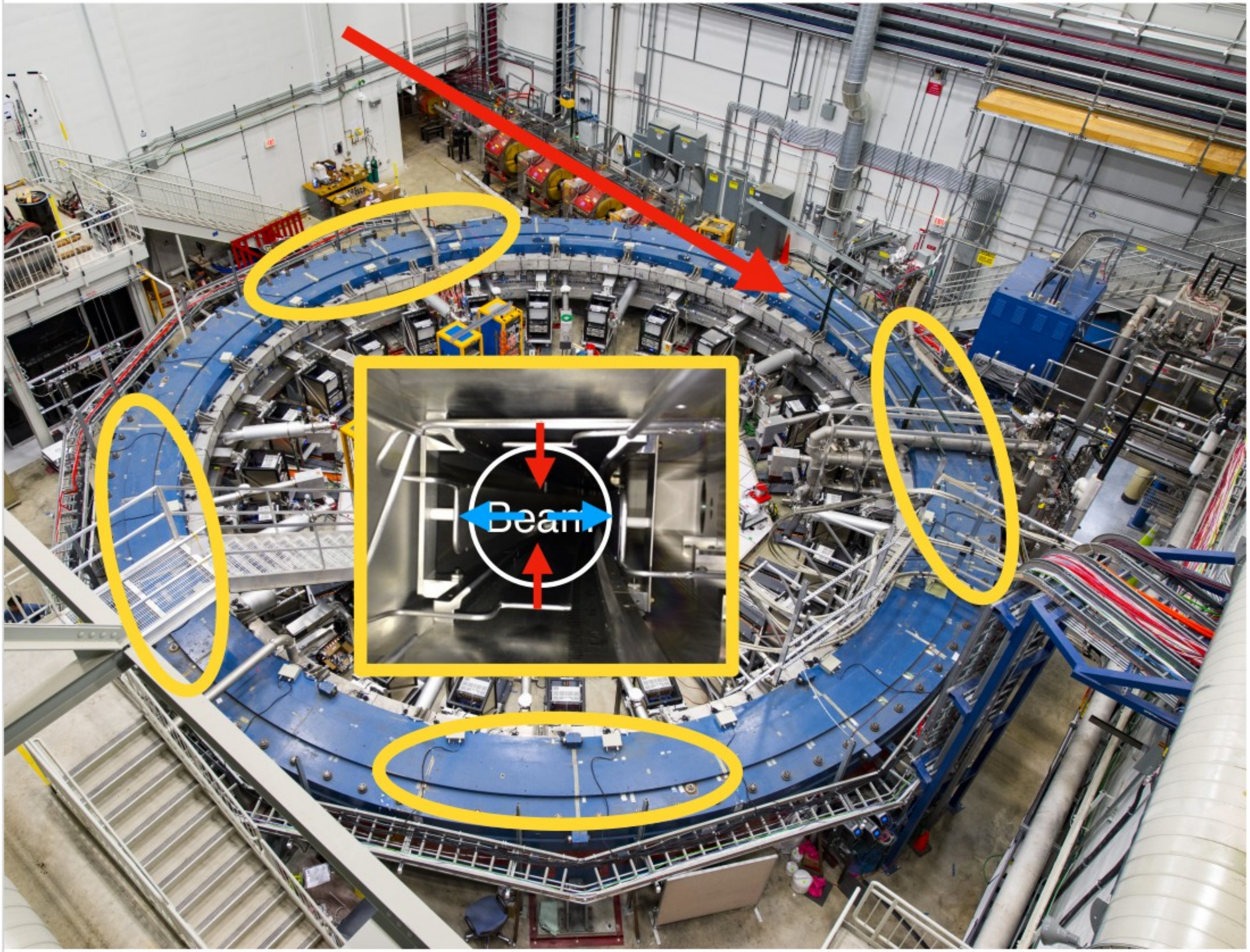

4 electrostatic quadrupoles force the muons to stay in the orbit plane, contrasting the betatron vertical oscillation and reducing the systematic effects due to a non perpendicular field

Corrections to the ideal formula

If the muon momentum is not perpendicular to the magnetic field and in presence of electric field the relation between ω_a and a_μ must be generalized as follows:

$$\vec{\omega}_a \equiv \vec{\omega}_s - \vec{\omega}_c = -\frac{q}{m_\mu}\left[a_\mu \vec{B} - a_\mu \left(\frac{\gamma}{\gamma+1}\right)(\vec{\beta}\cdot\vec{B})\vec{\beta} - \left(a_\mu - \frac{1}{\gamma^2-1}\right)\frac{\vec{\beta}\times\vec{E}}{c}\right]$$

Corrections to the ideal formula

If the muon momentum is not perpendicular to the magnetic field and in presence of electric field the relation between ω_a and a_μ must be generalized as follows:

$$\vec{\omega}_a \equiv \vec{\omega}_s - \vec{\omega}_c = -\frac{q}{m_\mu}\left[a_\mu \vec{B} - a_\mu \left(\frac{\gamma}{\gamma+1}\right)(\vec{\beta}\cdot\vec{B})\vec{\beta} - \left(a_\mu - \frac{1}{\gamma^2-1}\right)\frac{\vec{\beta}\times\vec{E}}{c}\right]$$

PITCH CORRECTION

We need a momentum perpendicular to the beam to keep the second term low. It's evaluated by the 'pitch correction'

Corrections to the ideal formula

If the muon momentum is not perpendicular to the magnetic field and in presence of electric field the relation between ω_a and a_μ must be generalized as follows:

$$\vec{\omega}_a \equiv \vec{\omega}_s - \vec{\omega}_c = -\frac{q}{m_\mu}\left[a_\mu \vec{B} - a_\mu \left(\frac{\gamma}{\gamma+1}\right)(\vec{\beta}\cdot\vec{B})\vec{\beta} - \left(a_\mu - \frac{1}{\gamma^2-1}\right)\frac{\vec{\beta}\times\vec{E}}{c}\right]$$

PITCH CORRECTION ELECTRIC FIELD CORRECTION

We need a momentum perpendicular to the beam to keep the second term low. It's evaluated by the 'pitch correction'

The third term is due to the electric field of the quadrupoles used to focus the beam vertically. Choosing for the muons the '**magic momentum**' p*~3.094 GeV/c, this term becomes 0. Deviations from the nominal magic momentum make the 'electric field' correction not null.

Magnetic field homogeneity

The 1.45 T field in the ring is provided by 3 superconducting coils
The C-shape allows the particles to be detected at the inner edge of the ring without appreciable energy loss
Using low-carbon steel **poles**, edge **shims**, steel **wedges** and a set of surface correction **coils** a field uniformity of **50 ppm** has been achieved!

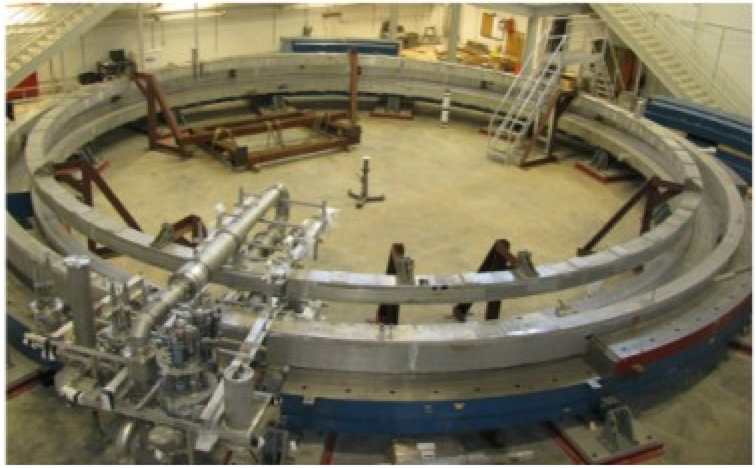

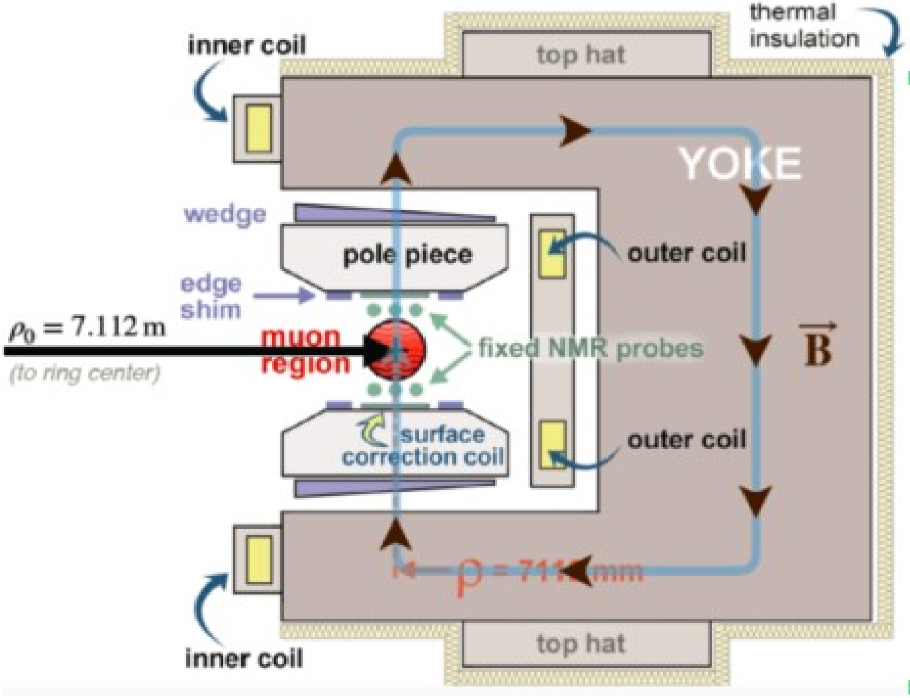

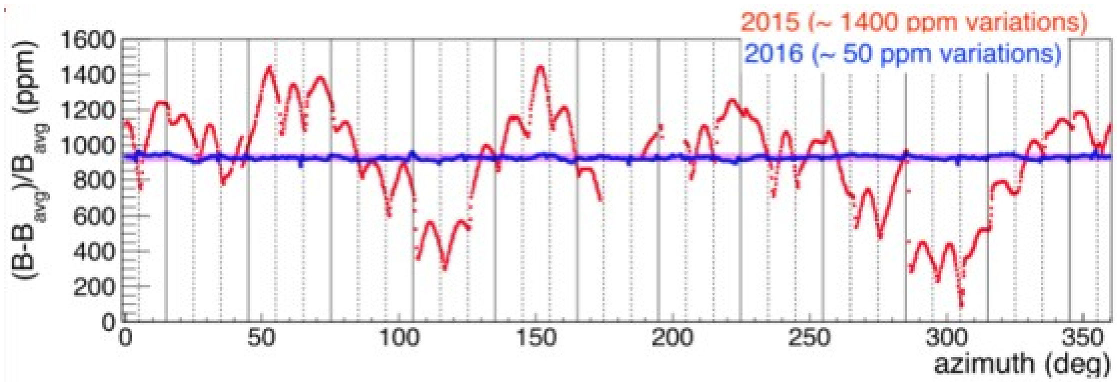

Precision measurement of the magnetic field

The measurement of the magnetic field is realized via an indirect measurement relying on other well measured quantitites:

$$a_\mu = \frac{\omega_a}{B}\frac{m_\mu}{q} = \frac{\omega_a}{\tilde{\omega}'_p(T_r)}\frac{m_\mu}{m_e}\frac{\mu_e(H)}{\mu_e}\frac{\mu'_p(T_r)}{\mu_e(H)}\frac{g_e}{2} \quad \text{with} \quad T_r = 34.7^o C$$

$\frac{m_\mu}{m_e}$ [22 ppb] : muonium hyperfine splitting [Phys. Rev. Lett. 82, 711 (1999)]

$\frac{\mu_e(H)}{\mu_e}$ [negligible] : QED calculation [Rev. Mod. Phys. 88 035009 (2016)]

$\frac{\mu'_p(T_r)}{\mu_e(H)}$ [10.5 ppb] : precession in water sample [Metrologia 13, 179 (1977)]

g_e [0.28 ppt] : precession in 1e cyclotron [Phys. Rev. A 83, 052122 (2011)]

total: **25 ppb**

Precision measurement of the magnetic field

The measurement of the magnetic field is realized via an indirect measurement relying on other well measured quantitites:

$$a_\mu = \frac{\omega_a}{B}\frac{m_\mu}{q} = \boxed{\frac{\omega_a}{\tilde{\omega}'_p(T_r)}}\frac{m_\mu}{m_e}\frac{\mu_e(H)}{\mu_e}\frac{\mu'_p(T_r)}{\mu_e(H)}\frac{g_e}{2} \quad \text{with} \quad T_r = 34.7^oC$$

$\frac{m_\mu}{m_e}$ [22 ppb] : muonium hyperfine splitting [Phys. Rev. Lett. 82, 711 (1999)]

$\frac{\mu_e(H)}{\mu_e}$ [negligible] : QED calculation [Rev. Mod. Phys. 88 035009 (2016)]

$\frac{\mu'_p(T_r)}{\mu_e(H)}$ [10.5 ppb] : precession in water sample [Metrologia 13, 179 (1977)]

g_e [0.28 ppt] : precession in 1e cyclotron [Phys. Rev. A 83, 052122 (2011)]

total: **25 ppb**

The only thing to be measured by the experiment is the ratio:

$$R_\mu = \frac{\omega_a}{\tilde{\omega}'_p(T_r)}$$

where $\tilde{\omega}'_p(T_r)$ is the precession frequency of protons shielded in water at the reference temperature T_r, averaged along the muon orbit.

Precision measurement of ω_p

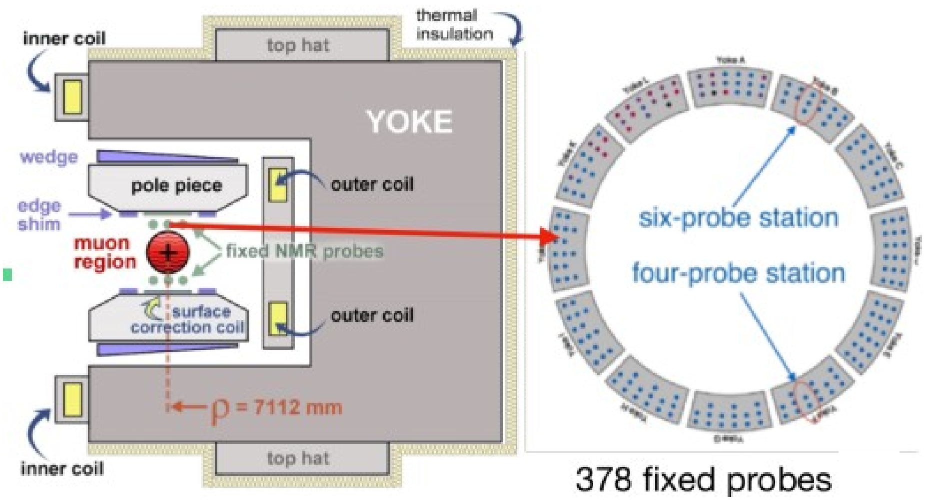

The proton precession frequency is continuously measured by 378 **fixed NMR probes** located above and below the beam all around the ring

Precision measurement of ω_p

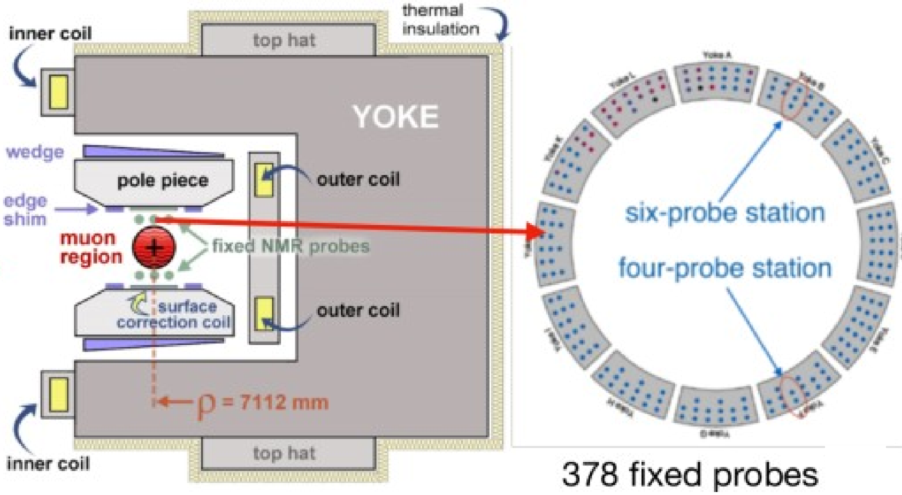

The proton precession frequency is continuously measured by 378 **fixed NMR probes** located above and below the beam all around the ring

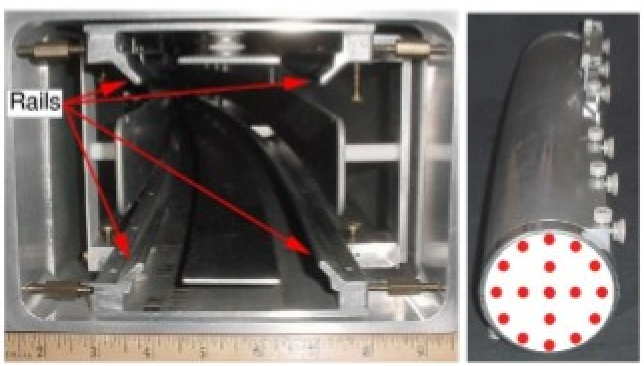

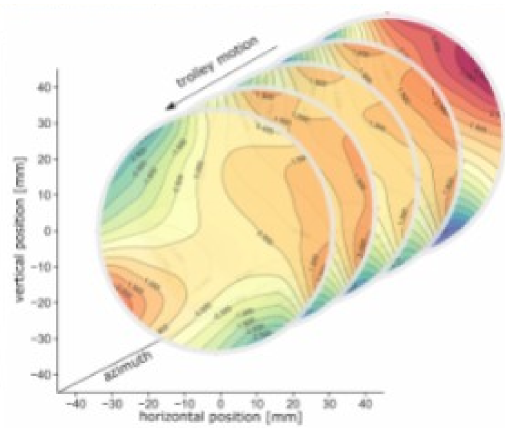

Each 2/3 days a **trolley** equipped with 17 petroleum jelly NMR probes is moved around the ring to provide continuous 2D maps

Precision measurement of ω_p

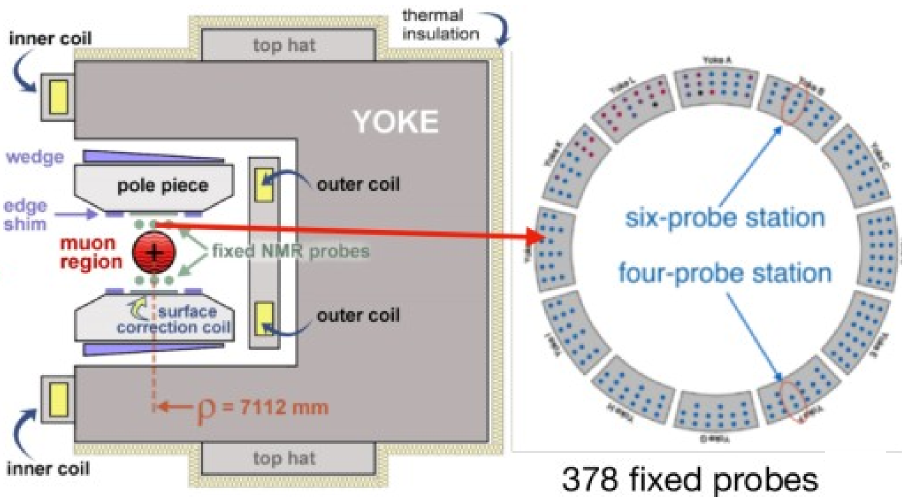

The proton precession frequency is continuously measured by 378 **fixed NMR probes** located above and below the beam all around the ring

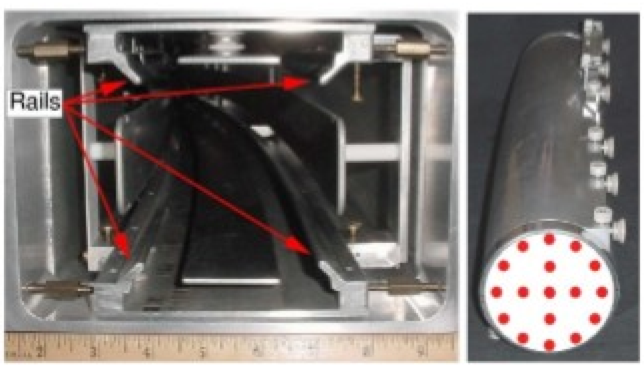

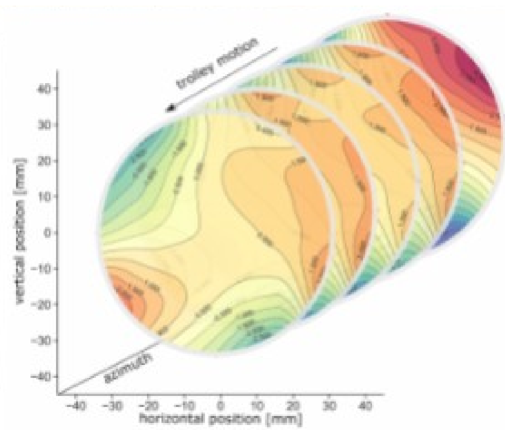

Each 2/3 days a **trolley** equipped with 17 petroleum jelly NMR probes is moved around the ring to provide continuous 2D maps

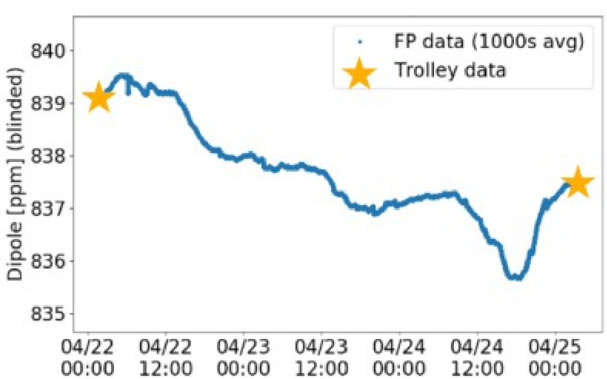

Fixed probes measurements are used to interpolate between trolley measurements Absolute calibration is provided (after unblinding) by H_2O probes calibrated at a known magnet

Tracking the beam position

The beam position is obtained by extrapolating back the tracks observed by 2 straw tube tracker stations placed around the ring

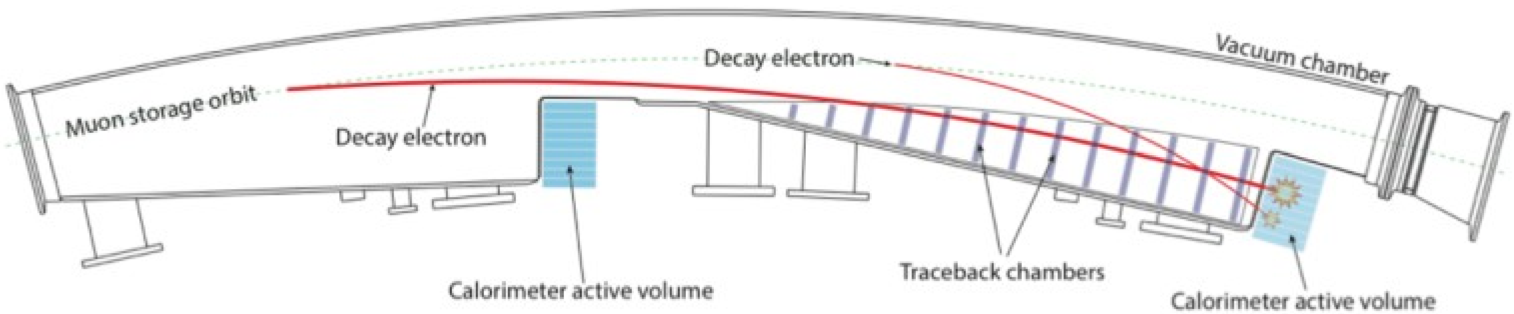

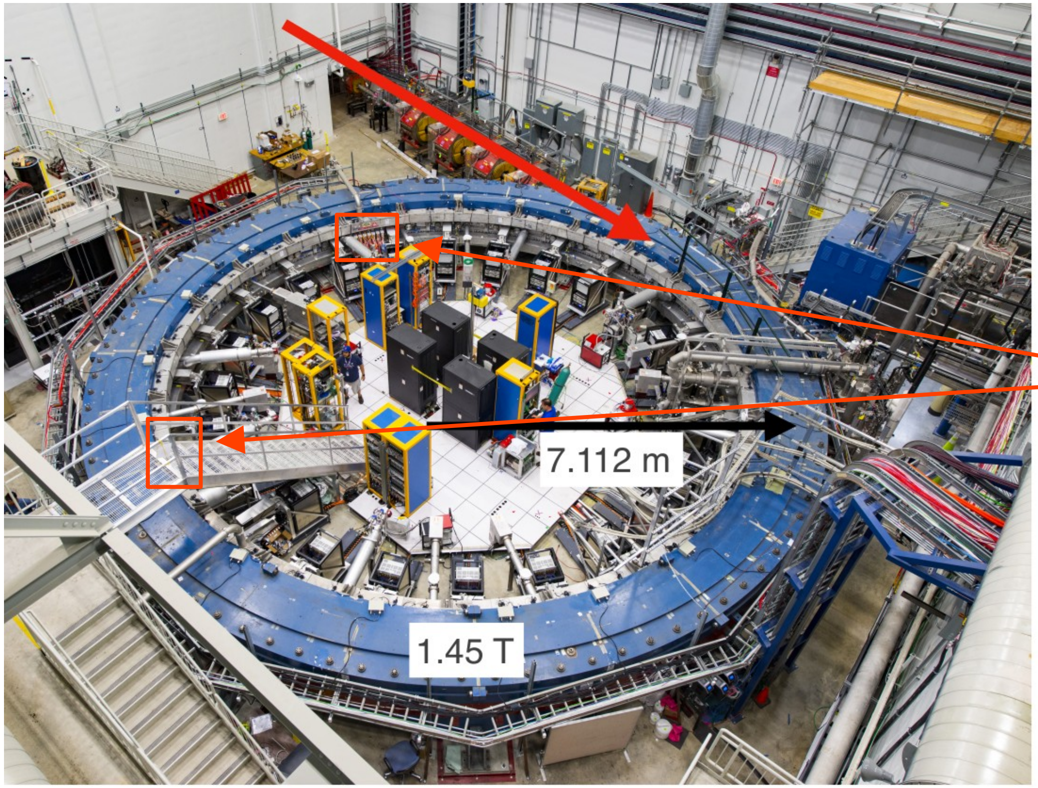

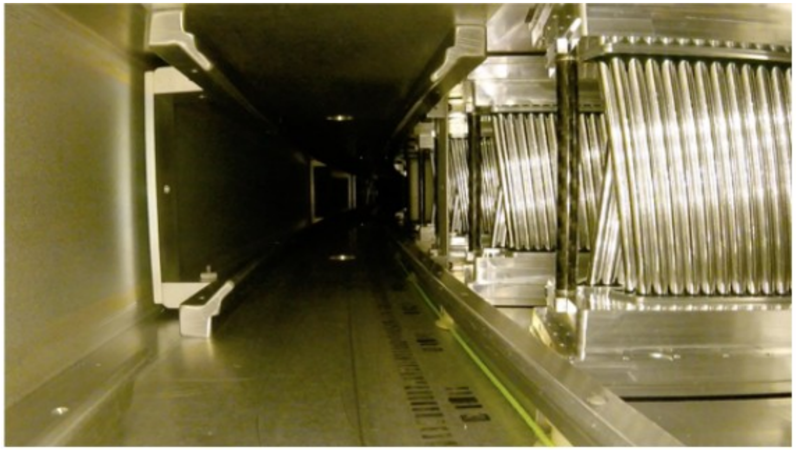

Betatron oscillations seen by the tracker

The beam oscillates and breathes

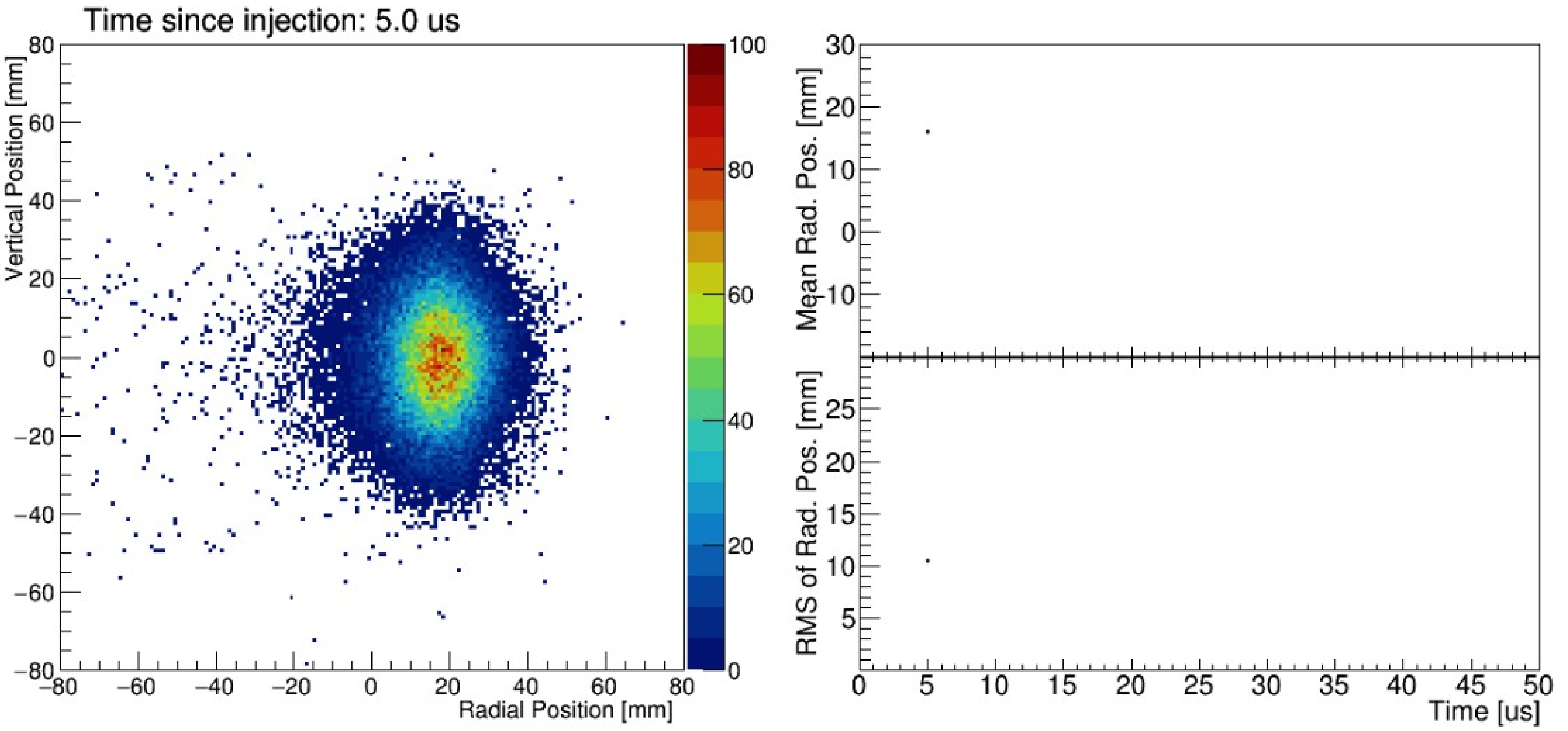

Betatron oscillations seen by the tracker

The beam oscillates and breathes:

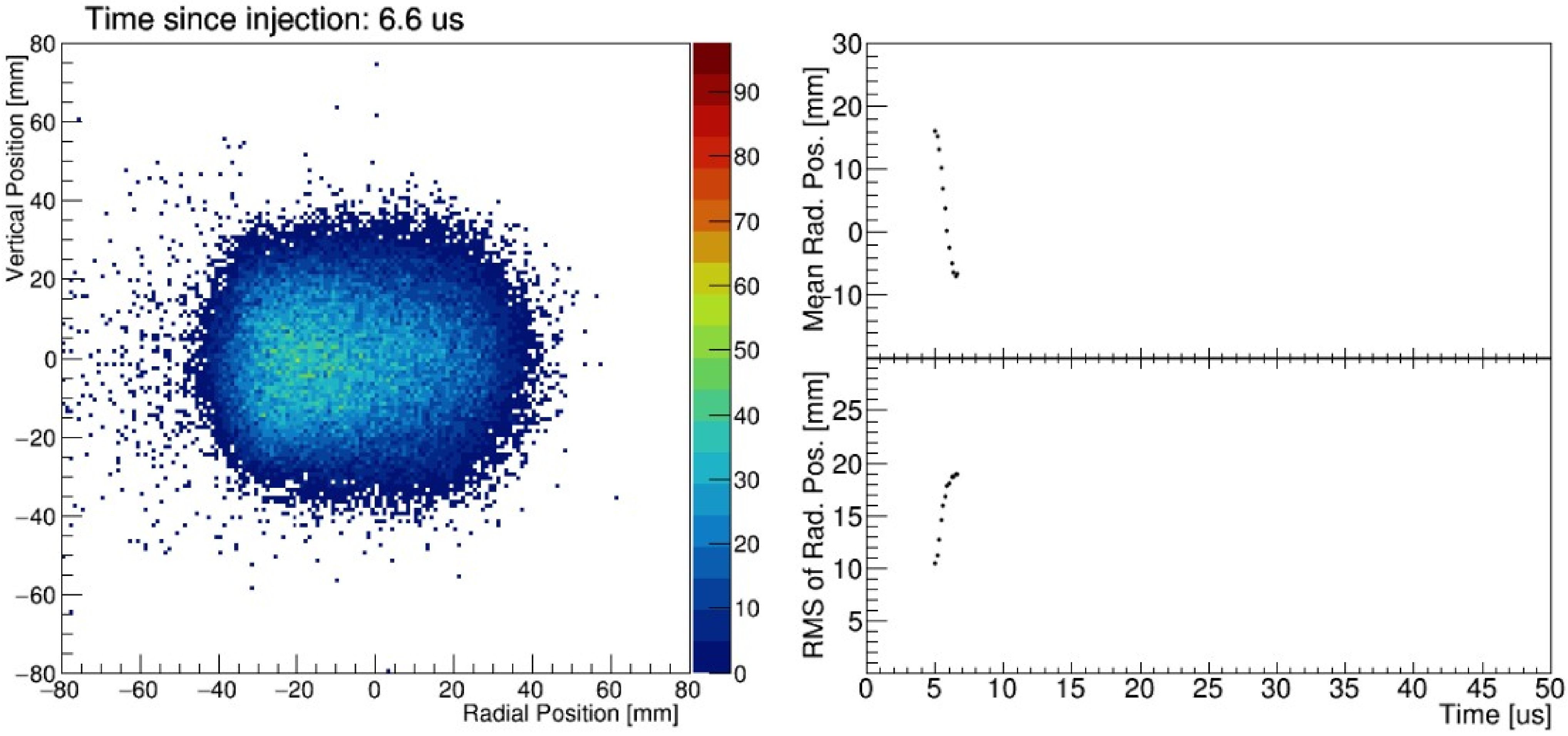

Betatron oscillations seen by the tracker

The beam oscillates and breathes:

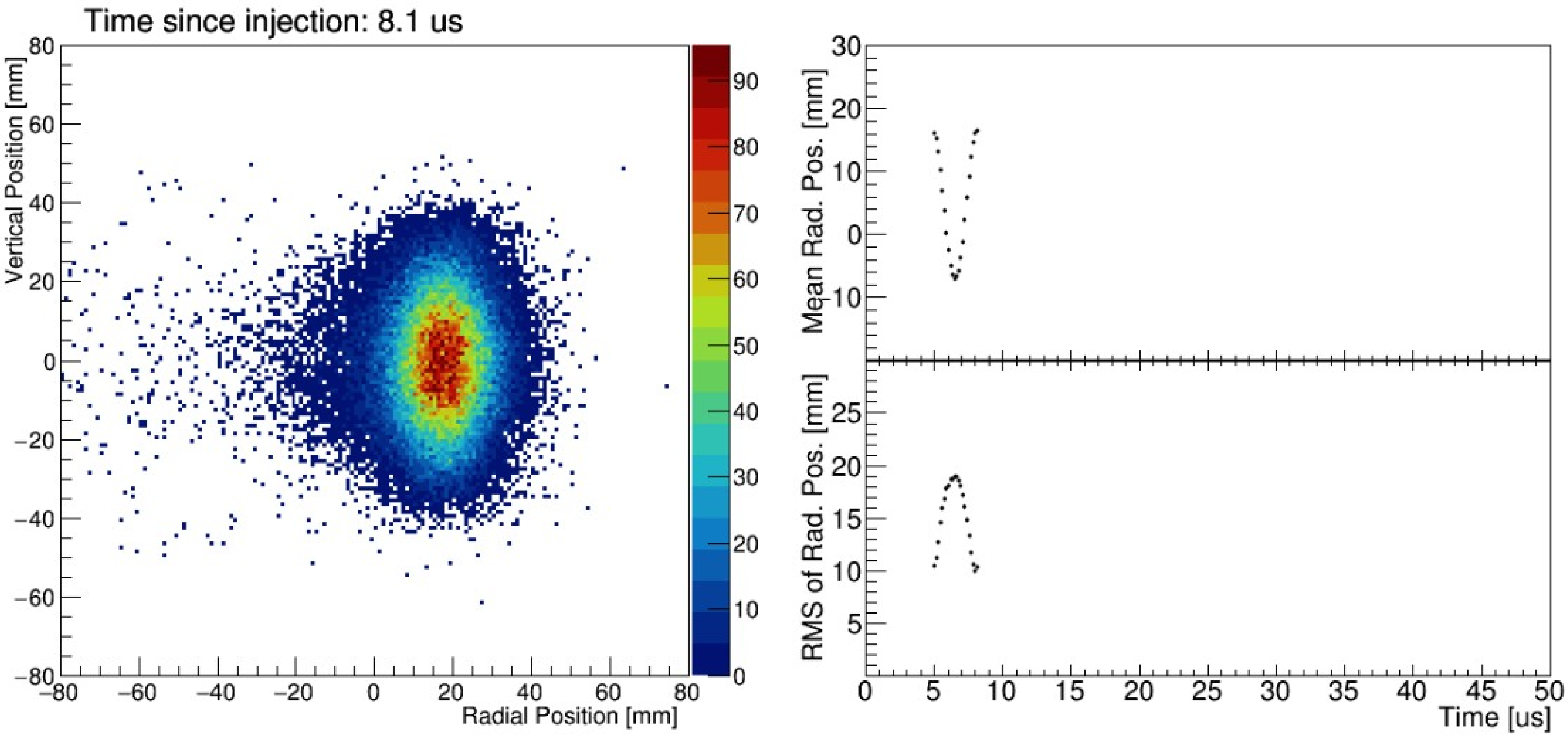

Betatron oscillations seen by the tracker

The beam oscillates and breathes:

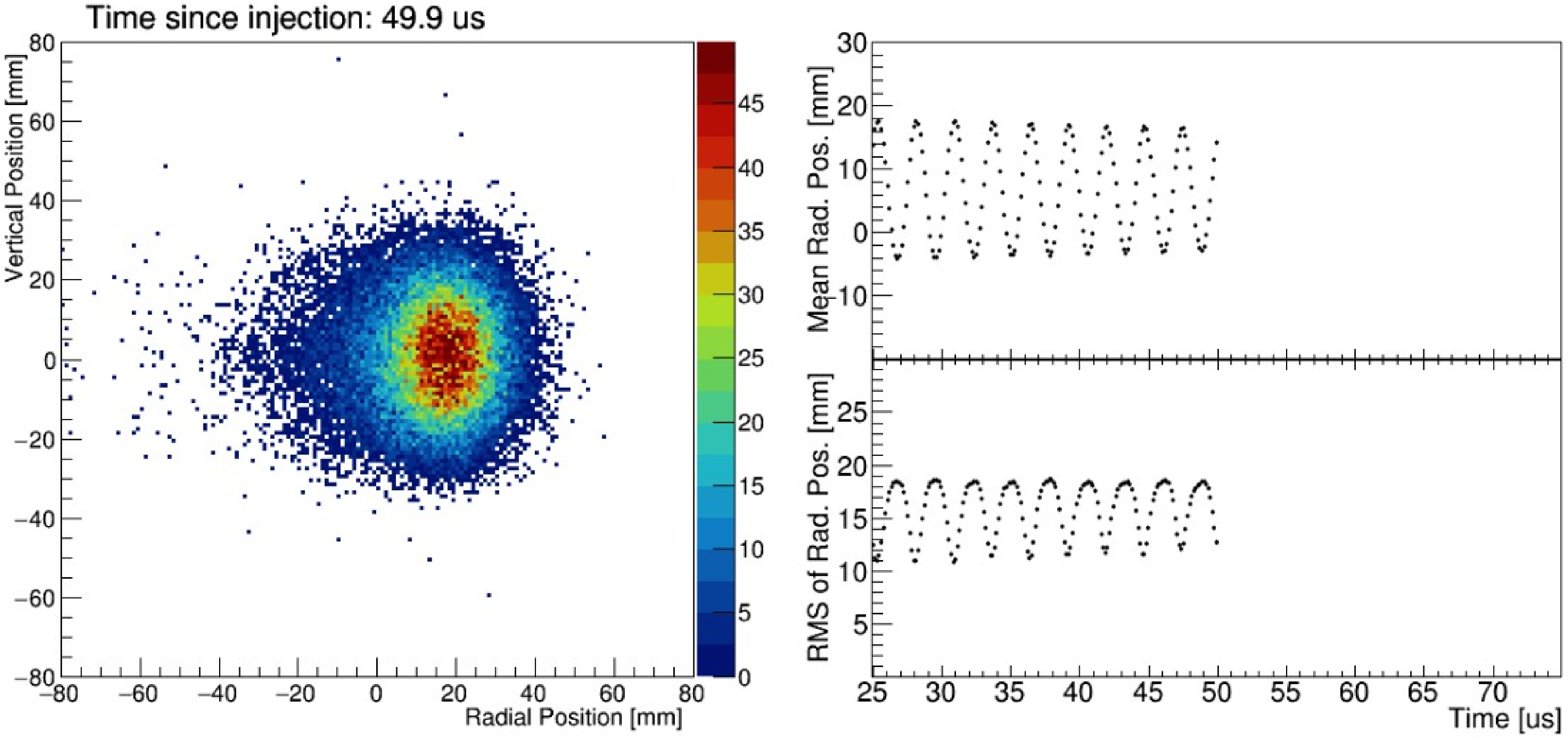

From ω'_p to $\tilde{\omega}'_p$

The average proton precession frequency is obtained by convoluting the field map measured by the probes and the average beam position obtained by tracker measurements and beam dynamics simulation

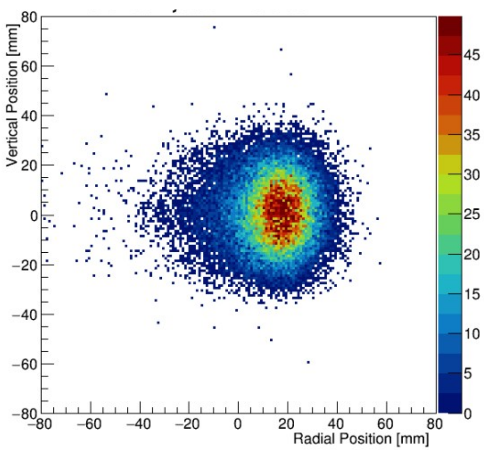

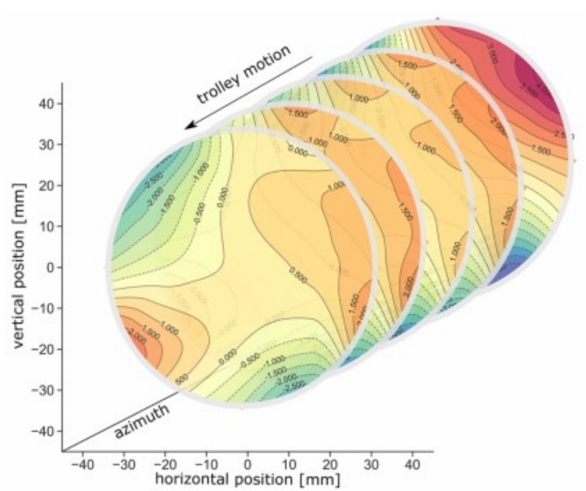

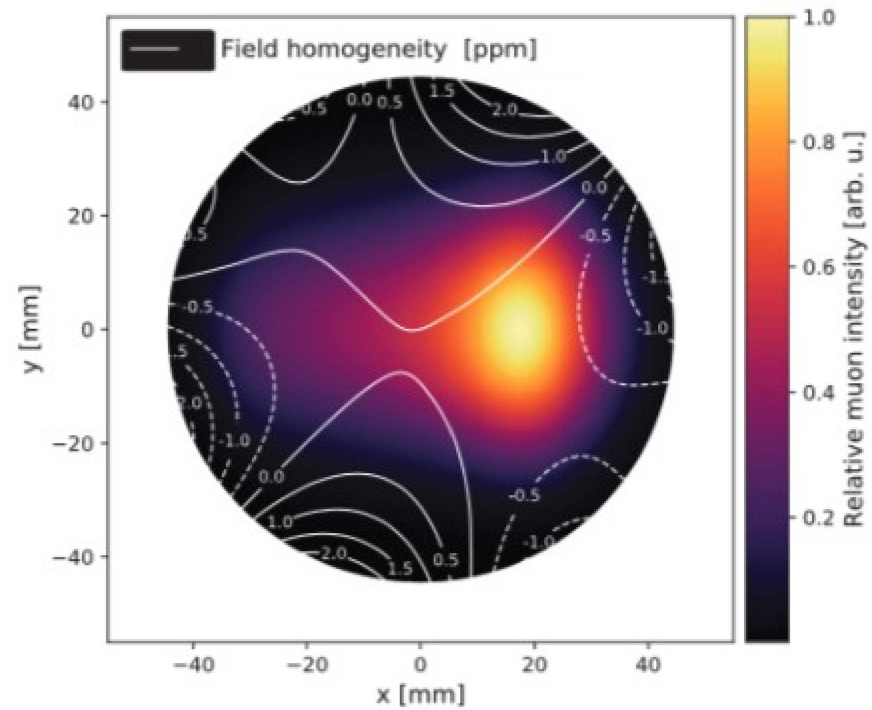

The total uncertainty on the convoluted field map is **56 ppb**

The electromagnetic calorimeters

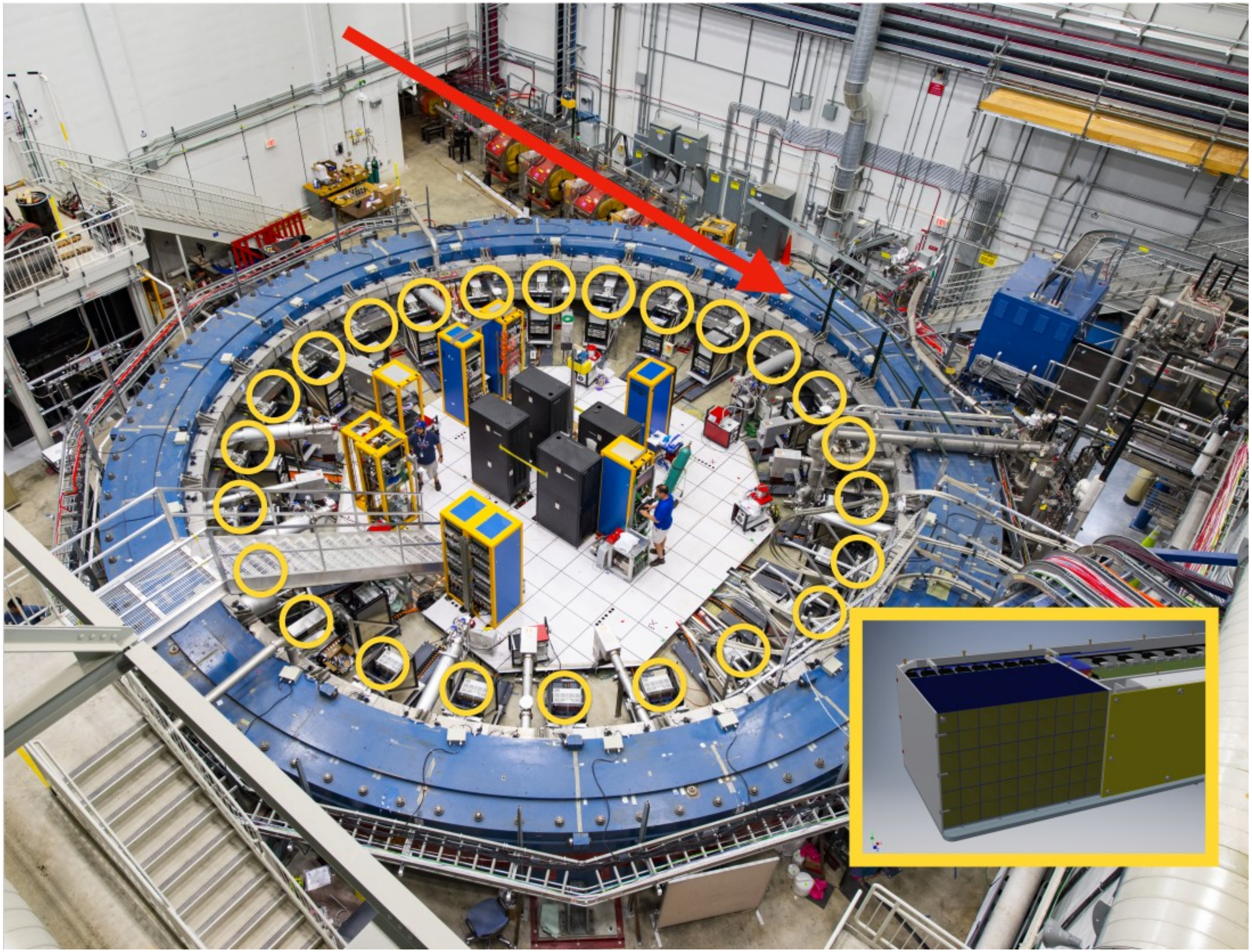

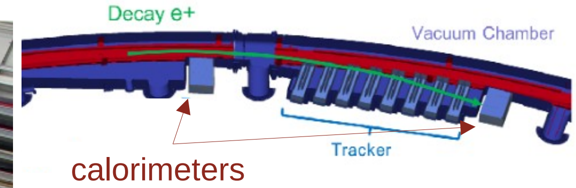

- 24 calorimeters
- 6x9 PbF_2 each
- individual SiPM readout
- 800 MHz digitizers
- no digitization threshold
- very low (50 MeV on any channel) trigger threshold

Positron time and energy reconstruction

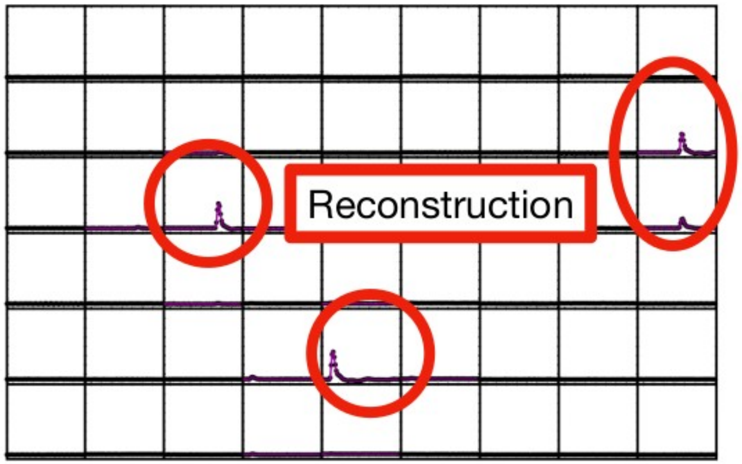

- SiPM gain known with a 10^{-4} precision thanks to a dedicated laser system
- clustering/pileup resolution

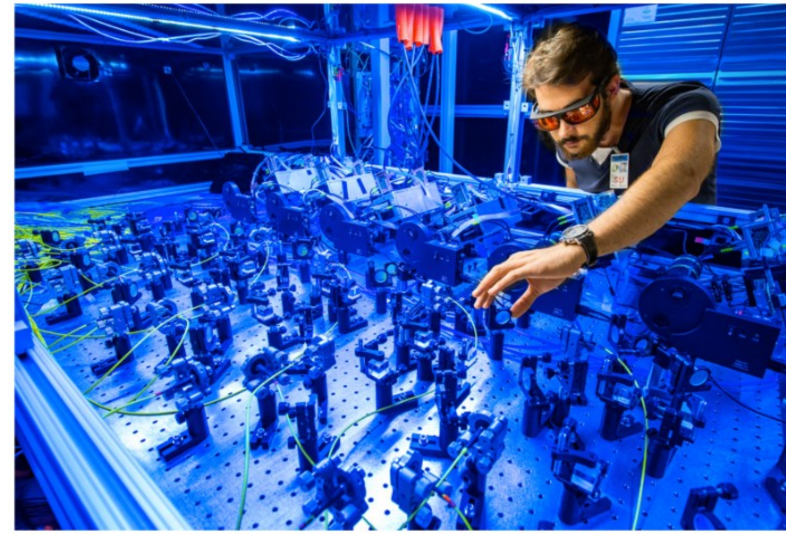

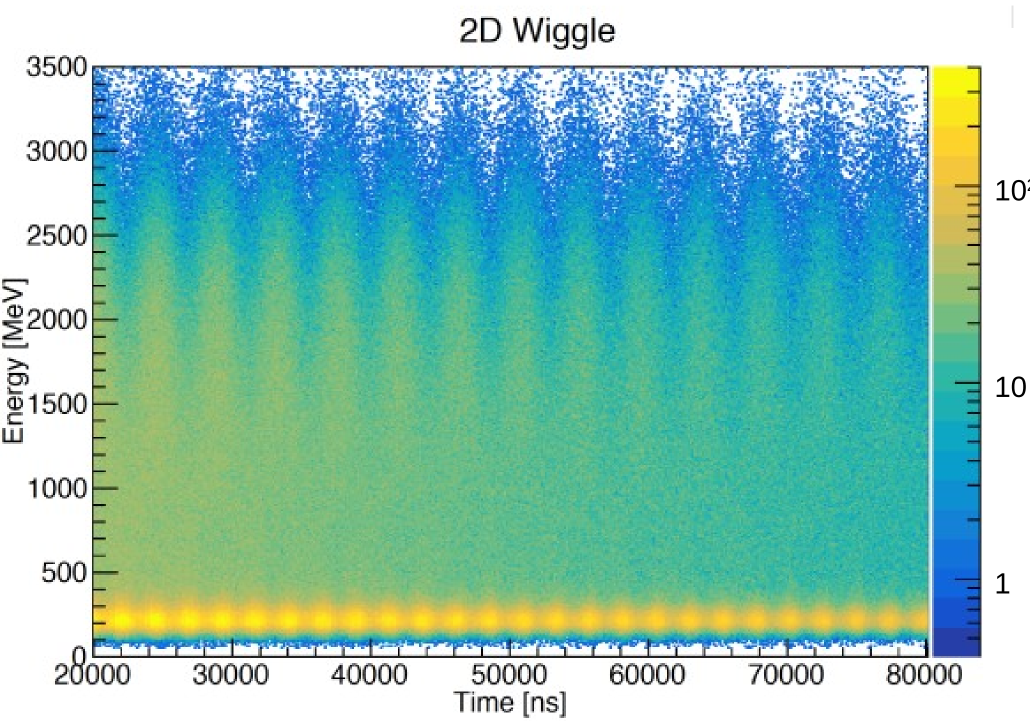

Run 1 ω_a analysis

4 techniques to check systematics:

- **Threshold (T) Method**: count positrons above threshold (1.7 GeV)
- **Asymmetry-Weighted (A) Method**: spectrum energy bins weighted by the spectrum asymmetry at that energies (high energies enhanced, 1.0 GeV threshold)
- **Ratio (R) Method**: exponential removed by making the ratio of close time bins
- **Integrated Charge (Q) Method**: sum of all calorimeter channels (no pileup error)

In total 11 analyses

Fitting the wiggle plot (first try)

Residuals of the wiggle plot fit with the 5 parameters function

$$f_5(t) = N_0 e^{-t/\tau}[1 - A\cos(\omega_a t + \phi)]$$

have an undesired oscillating behaviour

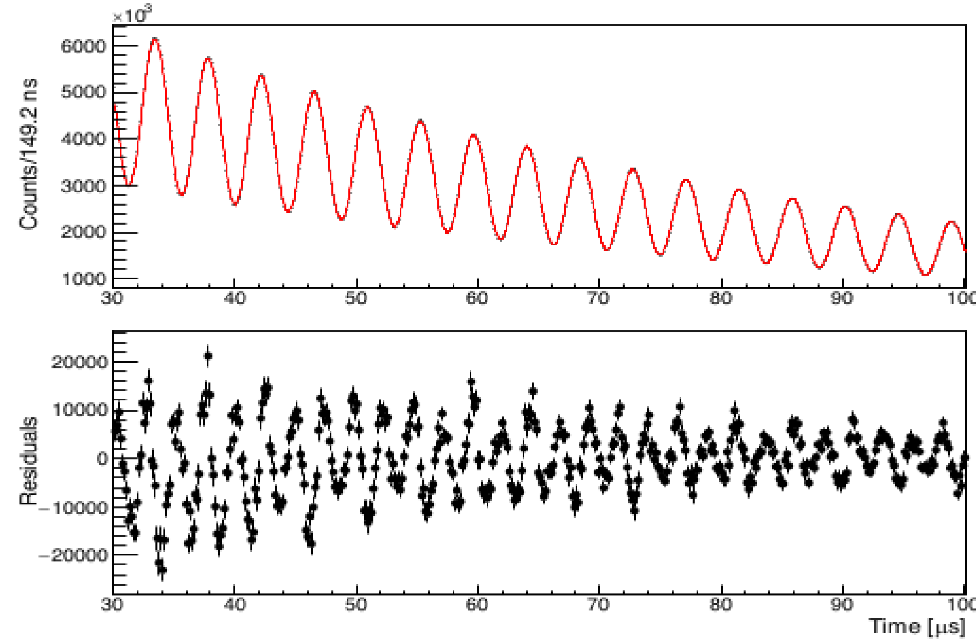

FFT analysis of fit residual peaks reveals peaks corresponding to beam dynamics frequencies (CBO and vertical oscillations)

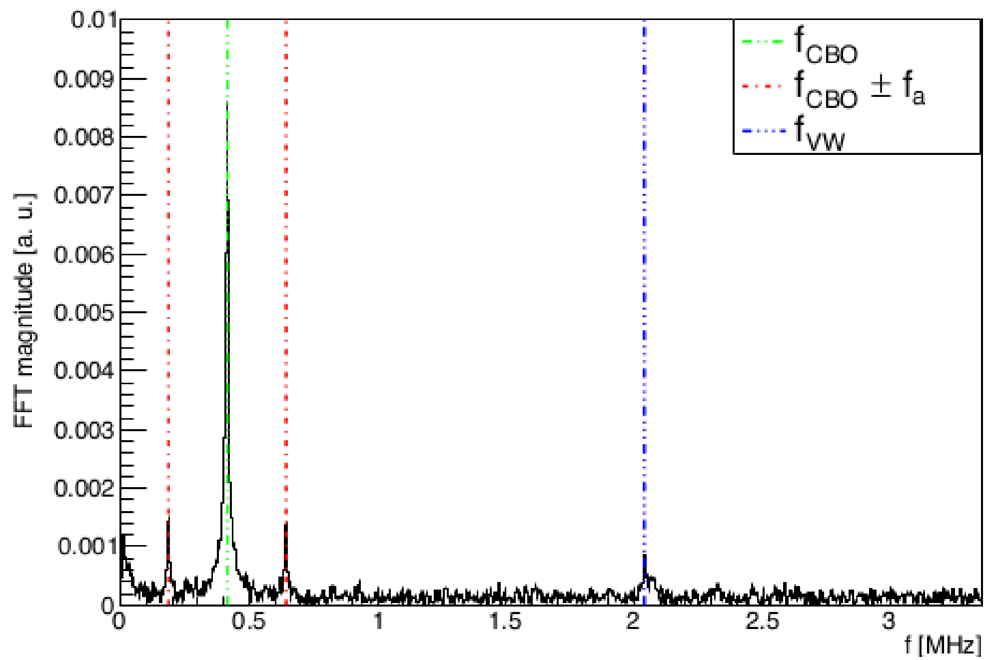

Fitting the wiggle plot

$$\boxed{N_0 e^{-\frac{t}{\tau}}\left(1 + A \cdot A_{BO}(t)\cos(\omega_a t + \phi \cdot \phi_{BO}(t))\right) \cdot N_{\rm CBO}(t) \cdot N_{\rm VW}(t) \cdot N_y(t) \cdot N_{\rm 2CBO}(t) \cdot J(t)}$$

$$A_{\rm BO}(t) = 1 + A_A \cos(\omega_{\rm CBO}(t) + \phi_A)e^{-\frac{t}{\tau_{\rm CBO}}}$$

$$\phi_{\rm BO}(t) = 1 + A_\phi \cos(\omega_{\rm CBO}(t) + \phi_\phi)e^{-\frac{t}{\tau_{\rm CBO}}}$$

$\omega_{CBO}, \omega_{2CBO}$ radial oscillations

$$N_{\rm CBO}(t) = 1 + A_{\rm CBO}\cos(\omega_{\rm CBO}(t) + \phi_{\rm CBO})e^{-\frac{t}{\tau_{\rm CBO}}}$$

$$N_{\rm 2CBO}(t) = 1 + A_{\rm 2CBO}\cos(2\omega_{\rm CBO}(t) + \phi_{\rm 2CBO})e^{-\frac{t}{2\tau_{\rm CBO}}}$$

$$N_{\rm VW}(t) = 1 + A_{\rm VW}\cos(\omega_{\rm VW}(t)t + \phi_{\rm VW})e^{-\frac{t}{\tau_{\rm VW}}}$$

$$N_y(t) = 1 + A_y\cos(\omega_y(t)t + \phi_y)e^{-\frac{t}{\tau_y}}$$

ω_y, ω_{VW} vertical oscillation:

Red = free parameters
Blue= fixed parameters

$$J(t) = 1 - k_{LM}\int_{t_0}^{t}\Lambda(t)dt$$

Lost muons

$$\omega_{\rm CBO}(t) = \omega_0 t + Ae^{-\frac{t}{\tau_A}} + Be^{-\frac{t}{\tau_B}}$$

$$\omega_y(t) = F\omega_{\rm CBO(t)}\sqrt{2\omega_c/F\omega_{\rm CBO}(t) - 1}$$

$$\omega_{\rm VW}(t) = \omega_c - 2\omega_y(t)$$

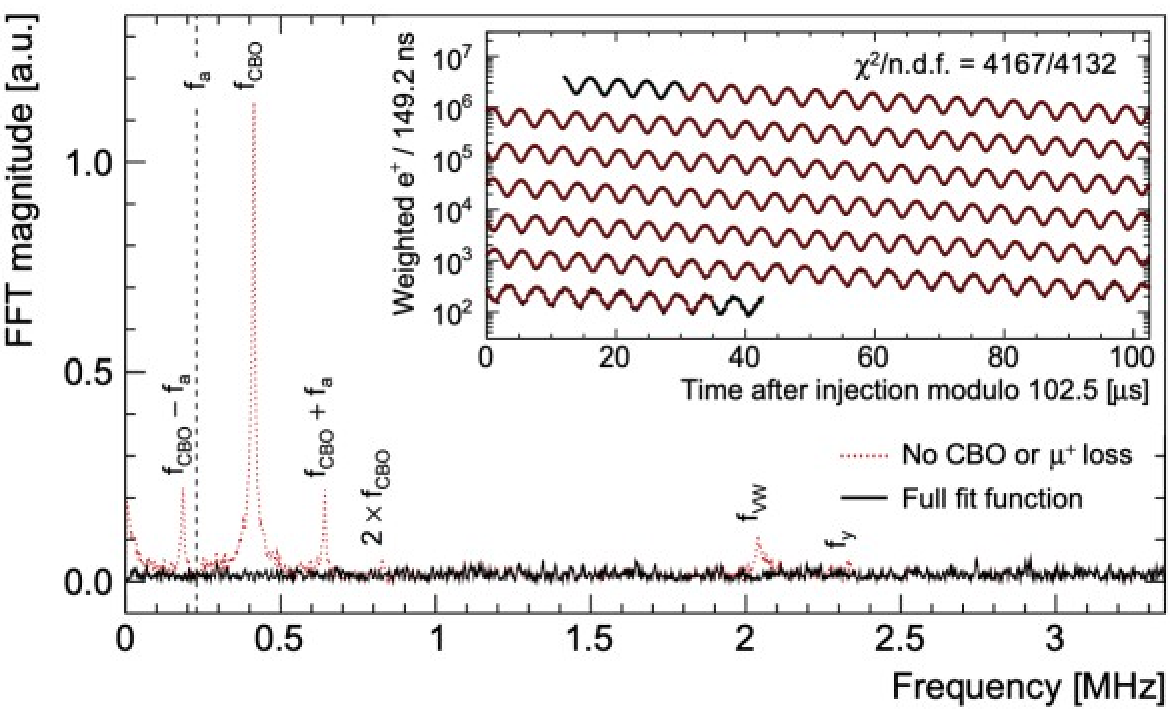

Including the beam oscillations in the fit function we have 22 parameters instead of 5. Some parameters (in blue) are obtained by separate analyses (lost muons, tracker analysis)

The 22 parameters fit gives a flat FFT

The measured value of ω_a (ω_a^m) is one of the fit parameters

Additional corrections

$$R_\mu = \frac{f_{clock}\omega_a^m(1 + C_e + C_p + C_{ml} + C_{pa})}{f_{calib}\tilde{\omega}_p'(T_r)(1 + B_k + B_q)}$$

$\mathbf{f_{clock}}$: clock frequency (**blinded** until all ω_a analyses and corrections are freezed)

C_e: **Electric field** effect for non magic muon momenta | 489 ± 53 ppb

C_p: **Pitch** correction due to vertical beam oscillations | 180 ± 13 ppb

C_{ml}: Time dependent phase shift due to **muon losses** correlated to muon momentum | -11 ± 5 ppb

C_{pa}: **Phase acceptance** effect: the time dependence of beam position (worsened by two damaged quadrupoles resistors replaced at the end of Run 1) causes a time dependence of muon phases detected by the calorimeters | -158 ± 75 ppb

Additional corrections

$$R_\mu = \frac{f_{clock}\omega_a^m(1 + C_e + C_p + C_{ml} + C_{pa})}{f_{calib}\tilde{\omega}'_p(T_r)(1 + B_k + B_q)}$$

f_{calib}: absolute probe calibration (blinded until all ω_p analyses are freezed)

± 56 ppb

B_k: **Transient kickers field** due to eddy currents induced by kicker pulses

-27± 37 ppb

B_q: **Transient quadrupoles field** produced by mechanical vibrations after the pulse

-17± 92 ppb

Errors summary

Quantity	Correction terms (ppb)	Uncertainty (ppb)
ω_a^m (statistical)	$\cdots$	434
ω_a^m (systematic)	$\cdots$	56
C_e	489	53
C_p	180	13
C_{ml}	−11	5
C_{pa}	−158	75
$f_{\text{calib}}\langle\omega_p(x,y,\phi) \times M(x,y,\phi)\rangle$	$\cdots$	56
B_k	−27	37
B_q	−17	92
$\mu'_p(34.7°)/\mu_e$	$\cdots$	10
m_μ/m_e	$\cdots$	22
$g_e/2$	$\cdots$	0
Total systematic	$\cdots$	157
Total fundamental factors	$\cdots$	25
Totals	544	462

The final unblinding

On Feb 25, 2021 the clock frequency has been unblided…

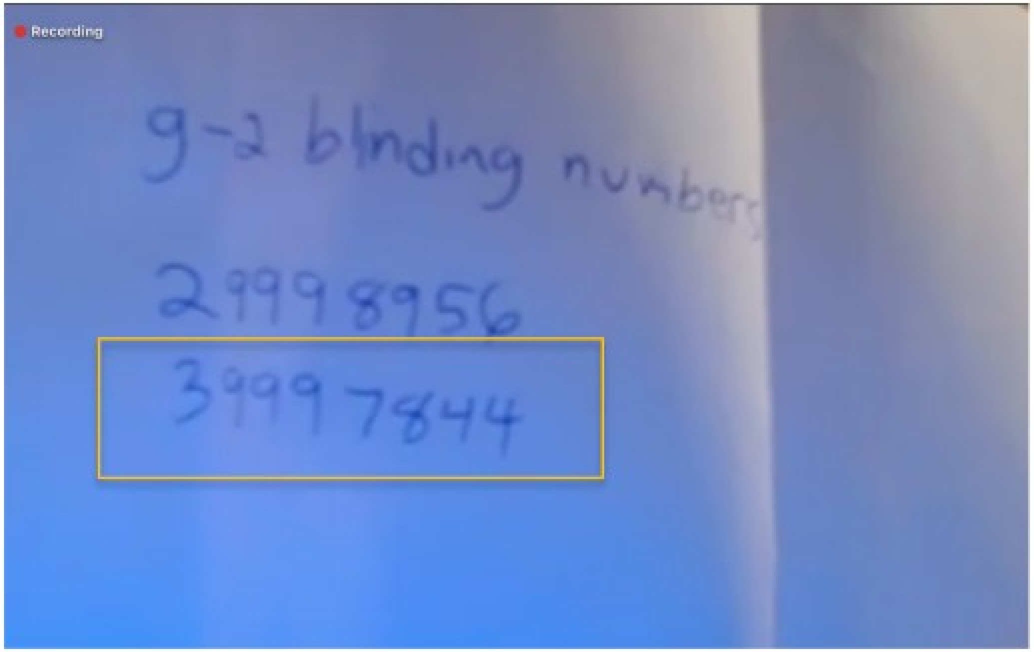

The final unblinding

On Feb 25, 2021 the clock frequency has been unblided…
… no more time for changes, inserting the corrected clock frequency in a program the final measurement has been set!

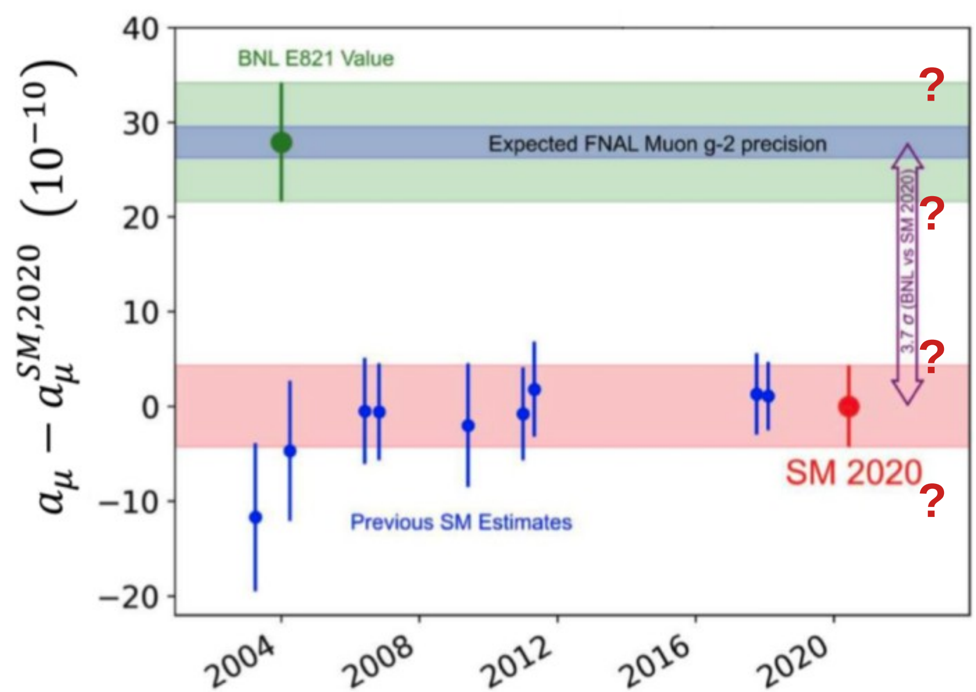

A new measurement of muon anomaly (Muon g-2 Run 1)

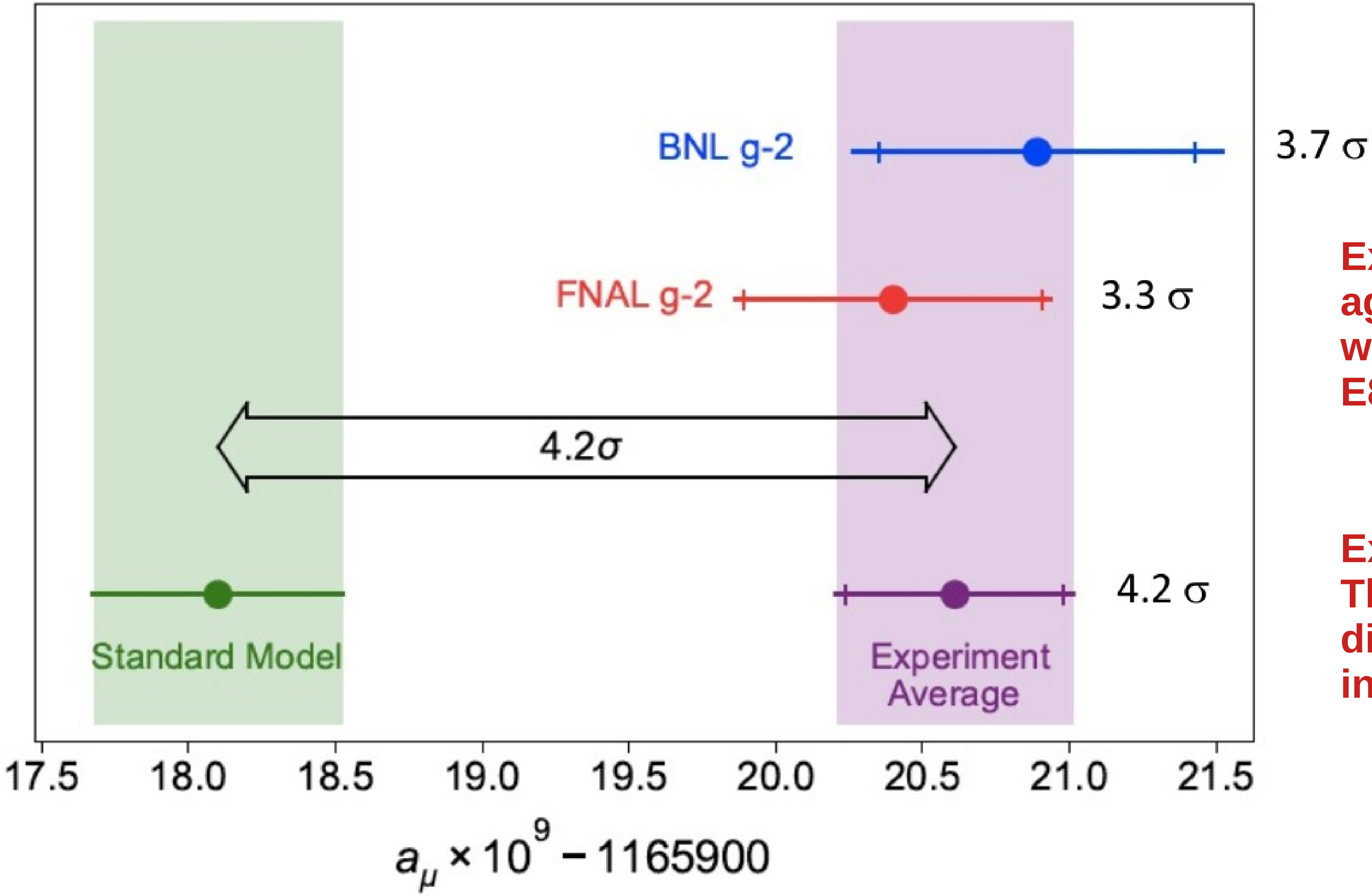

Excellent agreement with BNL E821 !!

Experiment-Theory discrepancy increased !!

$$a_\mu(\mathrm{FNAL}) = 116\,592\,040(54) \times 10^{-11} \quad (0.46\,\mathrm{ppm})$$

Four publications with all analysis details (2021)

PHYSICAL REVIEW ACCELERATORS AND BEAMS **24,** 044002 (2021)

Beam dynamics corrections to the Run-1 measurement of the muon anomalous magnetic moment at Fermilab

T. Albahri,

Beam dynamics

PHYSICAL REVIEW D **103,** 072002 (2021)

Editors' Suggestion | Featured in Physics

Measurement of the anomalous precession frequency of the muon in the Fermilab Muon $g-2$ Experiment

T. Albahri,

ω_a

PHYSICAL REVIEW A **103**, 042208 (2021)

Featured in Physics

Magnetic-field measurement and analysis for the Muon $g-2$ Experiment at Fermilab

T. Albahri,[39]

ω_p

PHYSICAL REVIEW LETTERS **126,** 141801 (2021)

Editors' Suggestion | Featured in Physics

Measurement of the Positive Muon Anomalous Magnetic Moment to 0.46 ppm

The result

B. Abi,[44] T. Albahri,[39] S. Al-Kilani,[36] D. Allspach,[7] L. P. Alonzi,[48] A. Anastasi,[11,a] A. Anisenkov,[4,b] F. Azfar,[44] K. Badgley,[7] S. Baeßler,[47,c] I. Bailey,[19,d] V. A. Baranov,[17] E. Barlas-Yucel,[37] T. Barrett,[6] E. Barzi,[7] A. Basti,[11,32] F. Bedeschi,[11] A. Behnke,[22] M. Berz,[20] M. Bhattacharya,[43] H. P. Binney,[48] R. Bjorkquist,[6] P. Bloom,[21] J. Bono,[7] E. Bottalico,[11,32] T. Bowcock,[39] D. Boyden,[22] G. Cantatore,[13,34] R. M. Carey,[2] J. Carroll,[39] B. C. K. Casey,[7] D. Cauz,[35,8] S. Ceravolo,[9] R. Chakraborty,[38] S. P. Chang,[18,5] A. Chapelain,[6] S. Chappa,[7] S. Charity,[7] R. Chislett,[36] J. Choi,[5] Z. Chu,[26,e] T. E. Chupp,[42] M. E. Convery,[7] A. Conway,[41] G. Corradi,[9] S. Corrodi,[1] L. Cotrozzi,[11,32] J. D. Crnkovic,[3,37,43] S. Dabagov,[9,f] P. M. De Lurgio,[1] P. T. Debevec,[37] S. Di Falco,[11] P. Di Meo,[10] G. Di Sciascio,[12] R. Di Stefano,[10,30] B. Drendel,[7] A. Driutti,[35,13,38] V. N. Duginov,[17] M. Eads,[22] N. Eggert,[6] A. Epps,[22] J. Esquivel,[7] M. Farooq,[42] R. Fatemi,[38] C. Ferrari,[11,14] M. Fertl,[48,16] A. Fiedler,[22] A. T. Fienberg,[48] A. Fioretti,[11,14] D. Flay,[41] S. B. Foster,[2] H. Friedsam,[7] E. Frlež,[47] N. S. Froemming,[48,22] J. Fry,[47] C. Fu,[26,e] C. Gabbanini,[11,14] M. D. Galati,[11,32] S. Ganguly,[37,7] A. Garcia,[48] D. E. Gastler,[2] J. George,[41] L. K. Gibbons,[6] A. Gioiosa,[29,11] K. L. Giovanetti,[15] P. Girotti,[11,32] W. Gohn,[38] T. Gorringe,[38] J. Grange,[1,42] S. Grant,[36] F. Gray,[24] S. Haciomeroglu,[5] D. Hahn,[7] T. Halewood-Leagas,[39] D. Hampai,[9] F. Han,[38] E. Hazen,[2]

New lattice calculations after the papers publishing

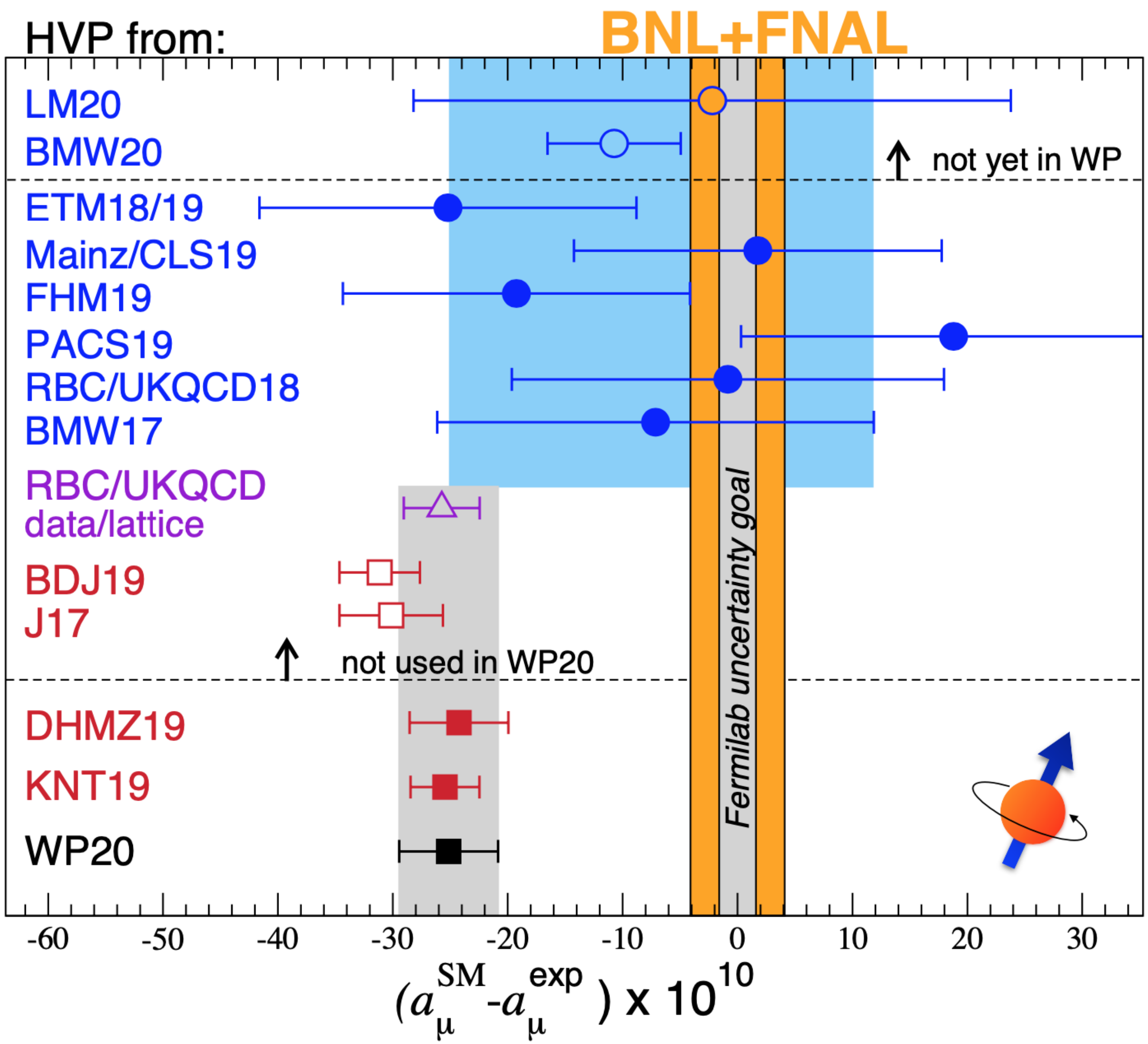

Tension between data driven and lattice ab initio HVP calculations still to be investigated...

Expected improvements from muon g-2

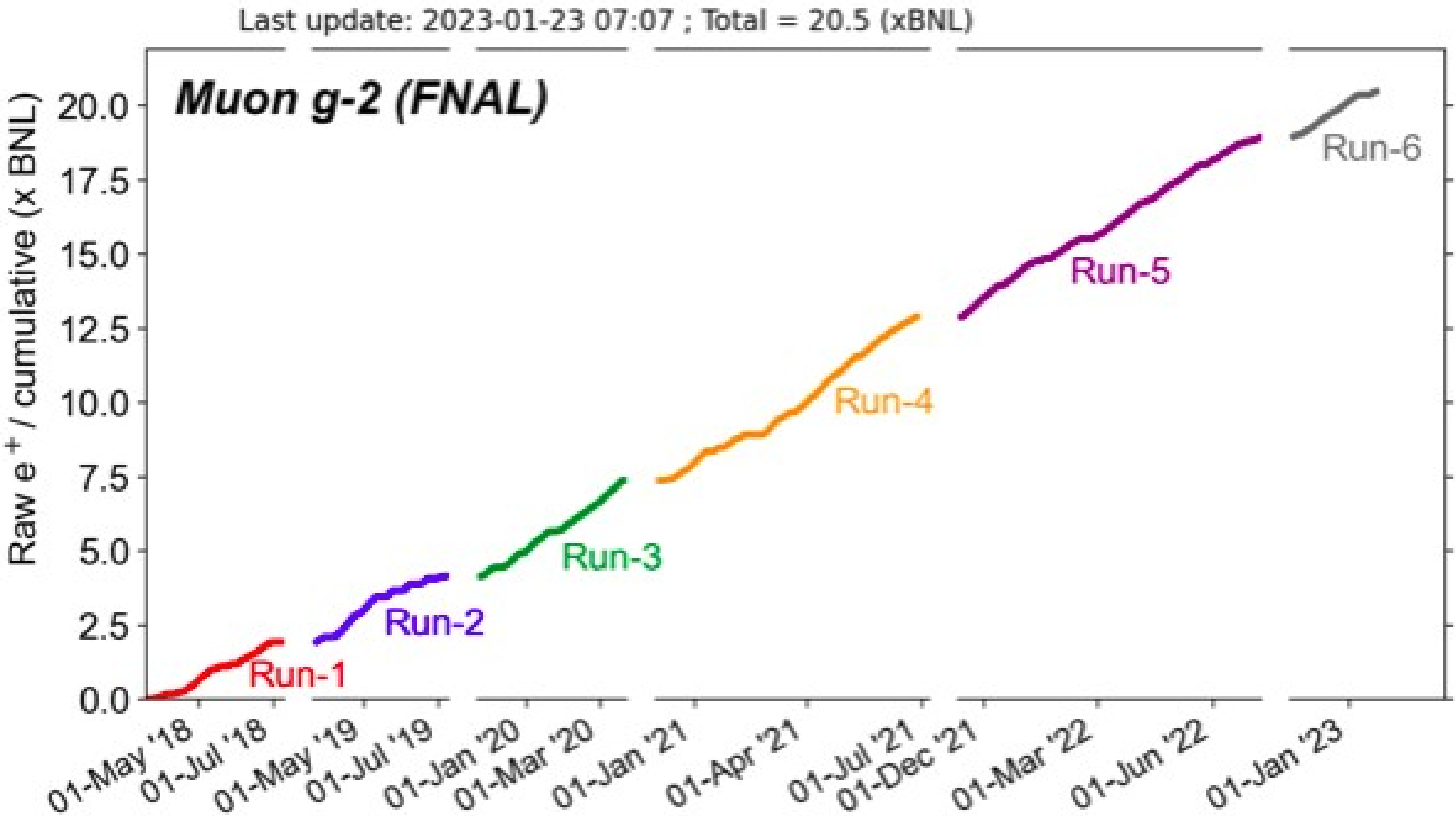

The measurement error is still statistically dominated
The statistical error goal of 140 ppb (21xBNL statistics) is almost reached!

Errors status and goals

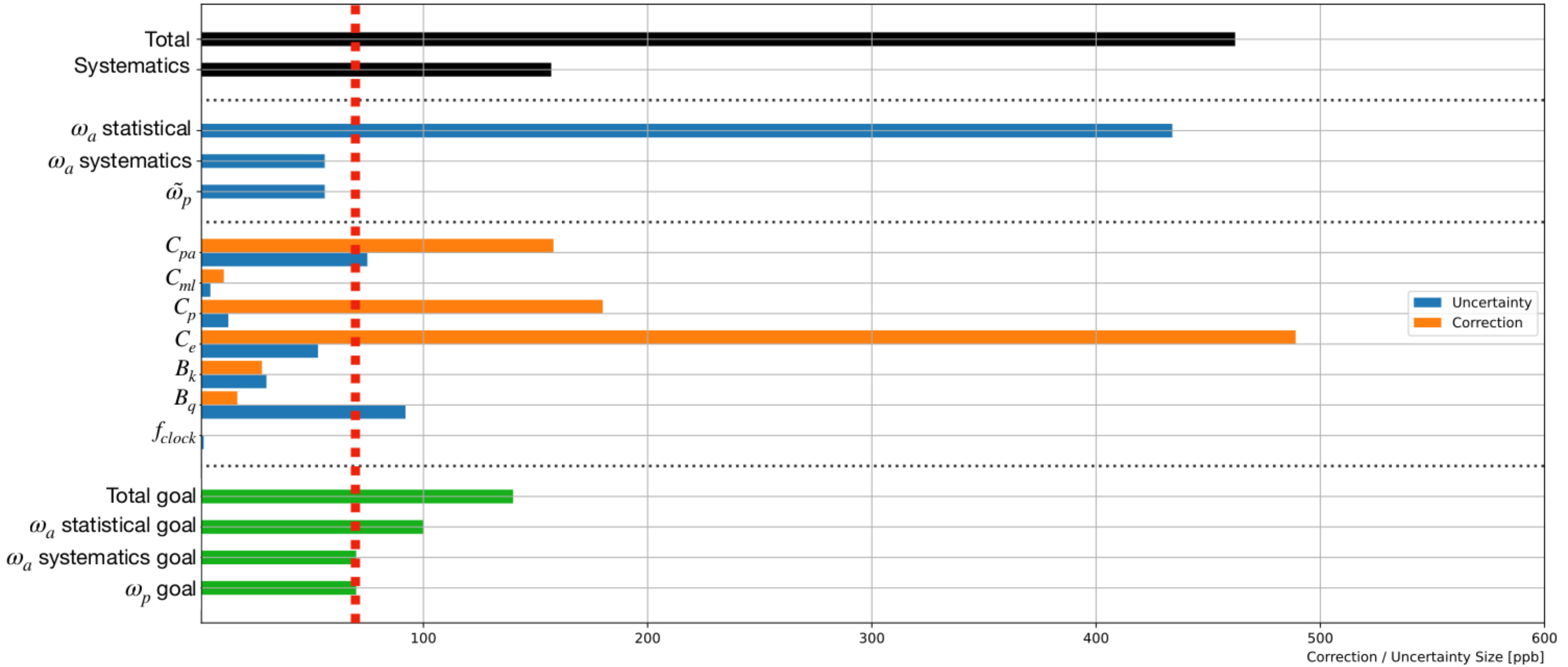

The total systematic error for Run 1 is 157 ppb, the goal is 100 ppb
Many systematic errors scale down with statistics
The largest systematic uncertainties for Run 1 come from phase acceptance and quadrupole transient field

Expected systematic improvement: quad cables

2 damaged quadrupole resistors where not reaching the nominal tension
-> replaced before Run 2

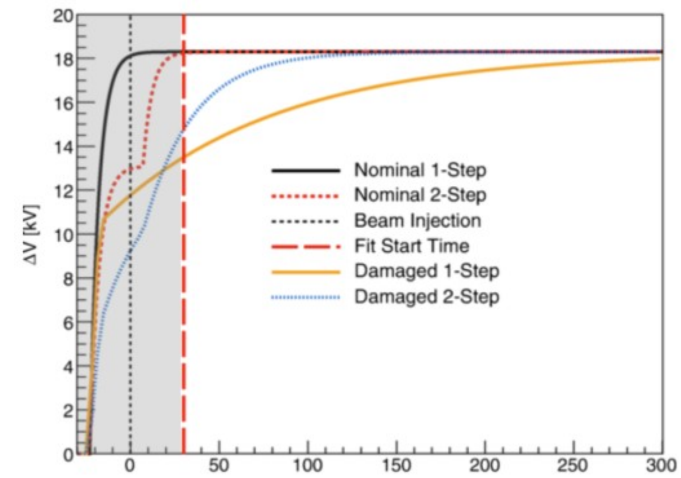

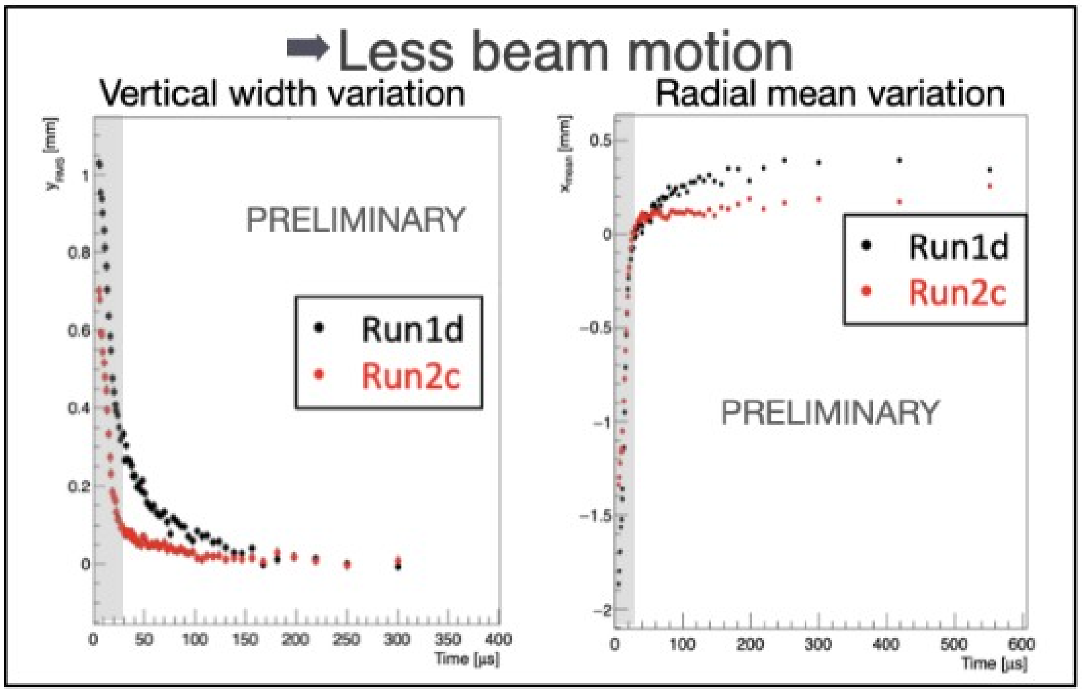

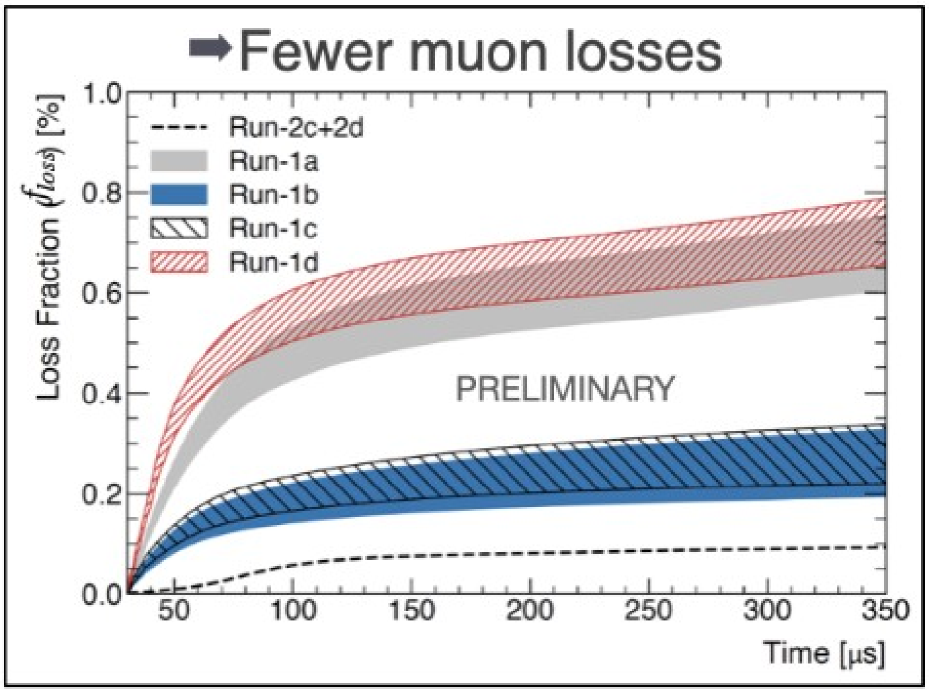

Expected systematic improvement: kicker cables

During Run 2 and Run 3 kicker cables replaced
→ able to reach the nominal voltage and place the beam at the center of nominal orbit

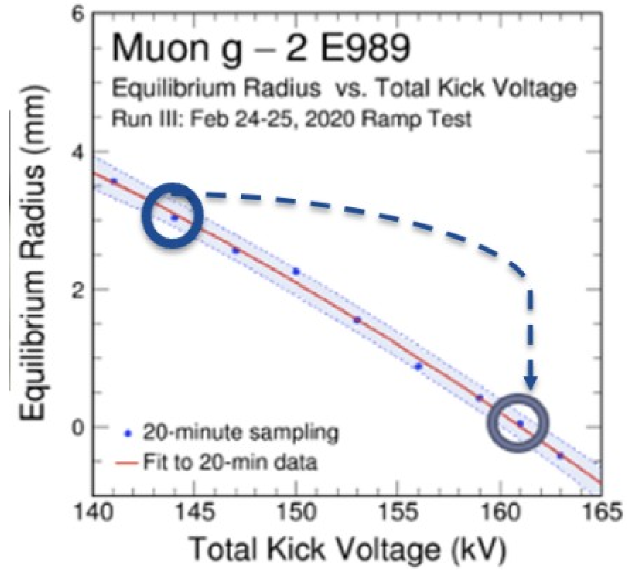

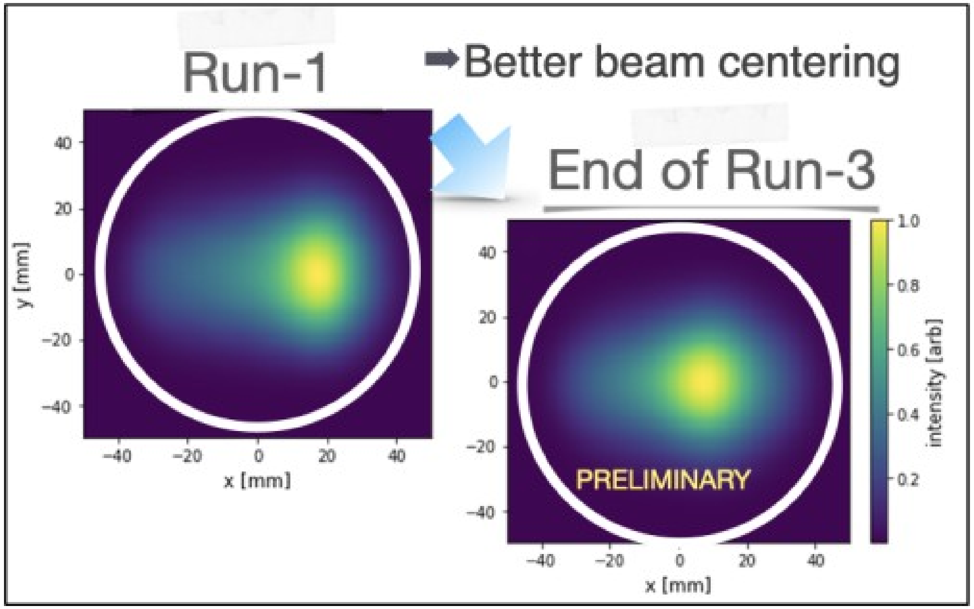

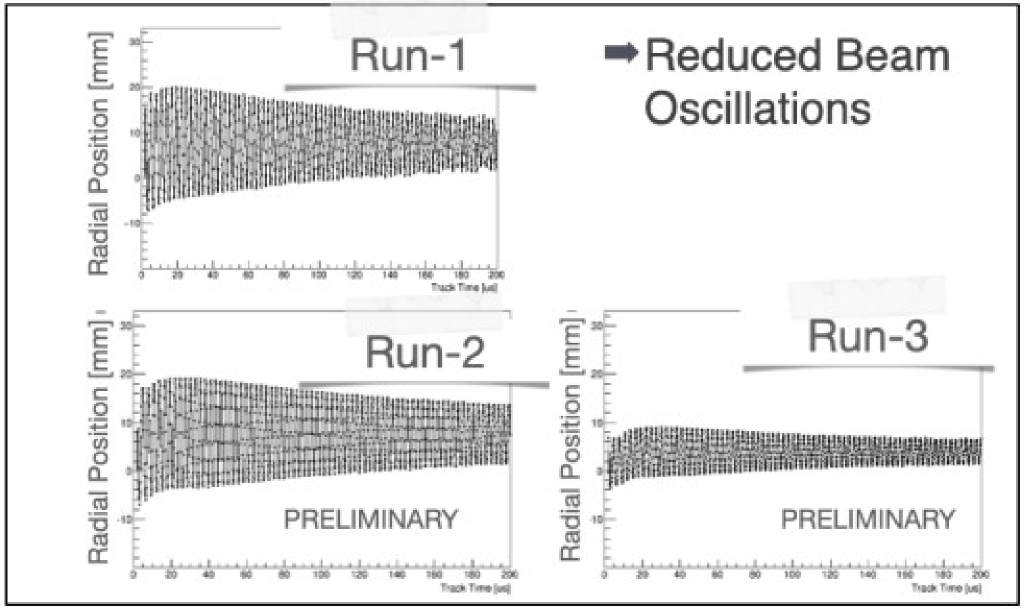

Expected systematic improvement: temperature

Before Run 2 magnet covered with a blanket
Before Run 3 Hall Temperature control

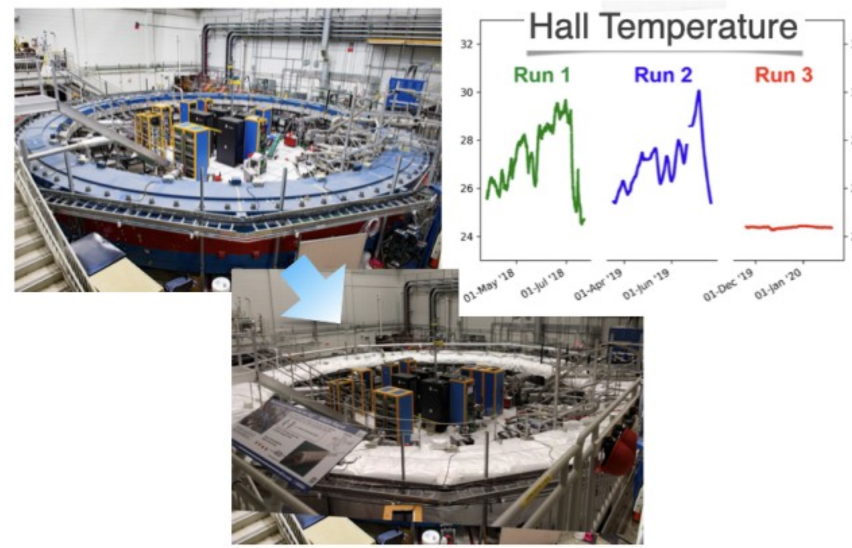

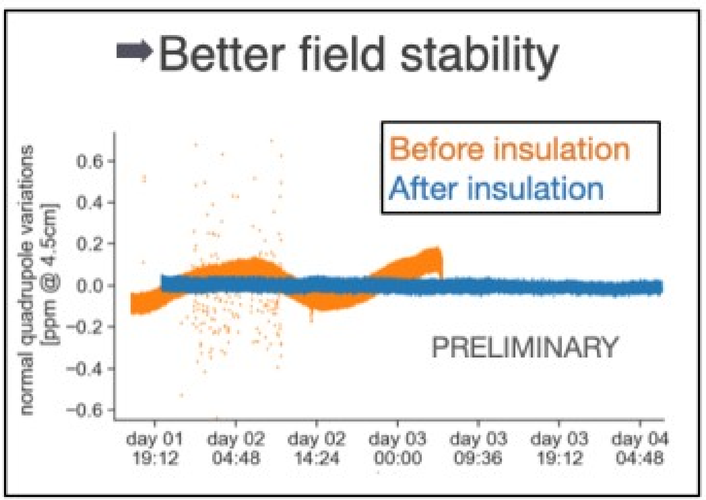

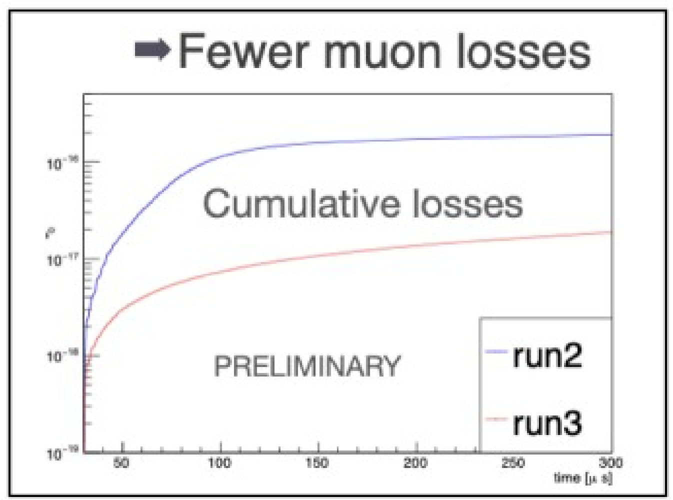

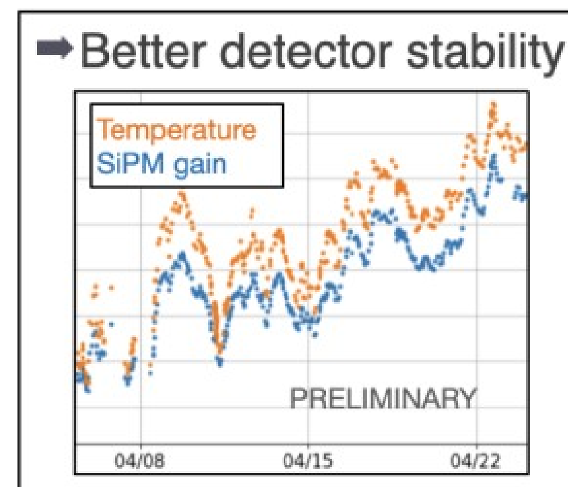

Other systematic improvements

ΔC_e : new detector to measure momentum-time correlation

ΔB_k : fiber magnetometer to measure kicker transient field

ΔB_q : PEEK probe to measure quad field transients

$\Delta \omega_a$: improved pileup separation algorithm

Δ_{CBO} : radiofrequency applied to quads to reduce horizontal oscillations

Summary and outlook

- The result from the analysis of the Run-1 data confirmed result from BNL experiment increasing the discrepancy with data driven theory calculations to 4.2σ (different for lattice calculation)
- Run-2 and Run-3 measurement should come out in few months: a factor 2 uncertainty reduction is expected
- Statistics goal of 21xBNL E821 will probably be reached in 1 month
- Current Run-6 will be the last one
- Improvements on hardware, ancillary measurements and analysis software make us confident to reach the experiment goal of 140 ppb total error

A tour of muon g-2 ring sitting on the trolley

Click to Start Muon g-2 trolley journey